Analysis of Proton Release in Oxygen Binding by Hemoglobin: Implications for the Cooperative Mechanism†

Angel Wai-mun Lee‡ and Martin Karplus*

Department of Chemistry, Harvard University, Cambridge, Massachusetts 02138

Claude Poyart and Elizabeth Bursaux

Unité 299, Institut National de la Santé et de la Recherche Médicale, 94275 Le Kremlin-Bicêtre, France

Received July 2, 1986; Revised Manuscript Received May 18, 1987

ABSTRACT: The relationship in hemoglobin between cooperativity (dependence of the Hill constant on pH) and the Bohr effect (dependence of the mean oxygen affinity on pH) can be described by a statistical thermodynamic model [Szabo, A., & Karplus, M. (1972) *J. Mol. Biol. 72*, 163–197; Lee, A., & Karplus, M. (1983) *Proc. Natl. Acad. Sci. U.S.A. 80*, 7055–7059]. In this model, salt bridges and other interactions serve to couple tertiary and quaternary structural changes. To test and refine the model, it is applied to the analysis of the pH dependence of the tetramer Adair constants corrected for statistical factors (K_{4i}', $i = 1$–4). Attention is focused on the proton release of the first ($\Delta H_1^+ = \partial \log K_{41}'/\partial$pH) and last ($\Delta H_4^+ = \partial \log K_{44}'/\partial$pH) oxygenation steps, where K_{4i}' are the Adair constants corrected for statistical factors. Measurements of ΔH_1^+ and ΔH_4^+ under carefully controlled conditions are reported, and good agreement between the model calculation and these experimental results is obtained. The salt bridges are found to be partially coupled to the ligation state in the deoxy quaternary structure; it is shown that a Monod–Wyman–Changeux-type model, in which the salt bridges are coupled only to quaternary structural change, is inconsistent with the data for ΔH_1. The significance of the present analysis for an evaluation of the Perutz mechanism [Perutz, M. F. (1970) *Nature (London) 228*, 726–734, 734–739] and other models for hemoglobin cooperativity is discussed.

The dependence of the mean oxygen affinity of hemoglobin on pH in the alkaline range (Bohr effect) has been recognized since Bohr first reported it in 1904 [see Antonini and Brunori (1971) and references cited therein]. Wyman (1948) used linkage relationships to show that the Bohr effect is equivalent to the proton release per heme on oxygenation and ascribed it to one ionizable group changing its pK_a from 7.93 to 6.68. Although it was generally assumed that oxygenation-induced conformational changes in the vicinity of the Bohr group are responsible for the lowering in its pK_a, the manner in which these changes occurred was not known until high-resolution X-ray crystallographic data for unliganded and liganded hemoglobins become available in the 1960s and 1970s (Fermi & Perutz, 1981, and references cited therein). The X-ray data demonstrated that there exist two quaternary structures (deoxy and oxy) for the tetramer and two tertiary structures (liganded and unliganded) for each individual chain. On the basis of a detailed analysis of the contacts present in the crystal structures, Perutz (1970a,b) proposed a stereochemical mechanism to explain hemoglobin cooperativity in which the stepwise increase in oxygen affinity is closely related to the Bohr effect. In this model, ionic interactions involving eight salt bridges (four per $\alpha\beta$ dimer) play a dominant role in coupling the ligand-induced tertiary structural changes and the relative stability of the quaternary structures. Since some of the salt bridges involve ionizable protons, the Perutz model also predicts the manner in which the Bohr protons are distributed among the different oxygenation steps. These Bohr groups have been identified experimentally from structural studies of mutant and modified hemoglobins (Perutz & Ten Eyck, 1971; Fermi & Perutz, 1981; Perutz et al., 1984) and from NMR (Kilmartin et al., 1973; Brown & Campbell, 1976), hydrogen-exchange (Ohe & Kajita, 1980; Matsukawa et al., 1984), and chemical reactivity (Garner et al., 1975; Van Beek, 1979) measurements.

The Perutz mechanism was translated into a statistical mechanical model (Szabo & Karplus, 1972, 1975, 1976) to provide a quantitative interpretation of the available thermodynamic data, including the Bohr effect. The Szabo–Karplus formulation is mathematically related to the Monod–Wyman–Changeux (MWC) model (Monod et al., 1965) in which cooperativity arises solely from a ligation-induced shift in the equilibrium between the deoxy (low affinity, T) and oxy (high affinity, R) quaternary structures. However, in contrast to the assumptions of the MWC model, ligation-induced changes in the tertiary structure can occur in the absence of a quaternary transition. From a fit of calculated oxygenation curves to data for oxygen binding in human hemoglobin at pH 7 and 9.1 (Roughton & Lyster, 1965), a set of values was determined for the free energy parameters appearing in the model. As a consequence of the assumptions of the model and of the choice of parameter values, a relationship was shown to exist between the Bohr effect (change of oxygen affinity with pH) and the degree of cooperativity (change of Hill constant with pH).

Despite the elegance of the Perutz mechanism and the success of the Szabo–Karplus (SK) model, the molecular basis of the Bohr effect and its relationship to cooperativity have not been completely resolved. This is due in part to the lack of structural and thermodynamic characterization of oxy-

† Supported in part by grants from the National Institutes of Health and from INSERM. A.W.L. was supported in part by the NIH Medical Scientist Training Program.

‡ Committee on Biophysics, Harvard University, Cambridge, MA 02138. Present address: National Heart, Lung, and Blood Institute, NIH, Bethesda, MD 20892.

0006-2960/88/0427-1285$01.50/0

genation intermediates that are present only in low concentrations due to the high cooperativity of the hemoglobin tetramer. Bunn and Guidotti (1972) concluded that the Bohr effect and cooperativity are independent phenomena because of the apparent insensitivity of the Hill constant to changes in pH. However, it is now clear (Lee & Karplus, 1983) that variations in n of the order of 0.2–0.5 over the pH 7–9 range are consistent with a partial but not complete coupling between cooperativity and the Bohr effect. Anderson reported intact salt bridges in the deoxy quaternary structure with liganded chains in aquomet-hemoglobin crystallized in an acrylamide gel (Anderson, 1973) and in carbonmonoxy-Hb Kansas in the presence of inositol hexaphosphate (Anderson, 1975), indicating that breaking of the salt bridges is not necessarily associated with the liganded tertiary structure.

Since the models considered in this paper focus on specific groups as the dominant contributors to the Bohr effect, it is important to evaluate the experimental evidence for their identity. This is particularly true because there has been considerable controversy on this point. We believe that the experimental data support the Perutz assignment as a useful approximation to a complex phenomenon. It should be noted, however, that the present models can be regarded as phenomenological in character with "effective" Bohr groups, analogous to those introduced in the early work of Wyman (1948, 1964). Thus, even if a misassignment of the Bohr groups has been made, the general conclusions of the analysis in the paper are still expected to be valid.

There are two related questions that have been raised concerning the Bohr group assignment. The first concerns the dominant role of β His-146 in the Bohr effect and the second the possibility that the Bohr effect involves many groups rather than the specific ones considered in the Perutz mechanism. Concerning β His-146, the history in the published literature is complex. The original NMR study in the presence of 0.2 M phosphate and 0.2 M Cl^- (Kilmartin et al., 1973), in which the resonances were assigned in both the deoxy and oxy forms and the pK_a difference was determined (pK_a = 8.0 in Hb; pK_a = 7.1 in HbCO), appears to be valid. Where there is an uncertainty is for unphysiological solution conditions of relatively low chloride in the absence of phosphate. Although the β His-146 assignment in Hb is clear, there appear to have been a series of misassignments for HbCO (Russu et al., 1980, 1982; Perutz et al., 1985a,b; Russu & Ho, 1986). At the present time (Clore, private communication; Perutz, private communication; Ho, private communication), the β His-146 resonance has not been assigned in HbCO, and so NMR measurements do not provide any information on the change of pK_a for this residue at low chloride in the absence of phosphate. In particular, NMR studies by Shih et al. (unpublished results) of the CO form of normal hemoglobin and hemoglobin Cowtown (β His-146 → Leu) did not show any differences in the histidine resonances that could be assigned to β His-146. Whatever the outcome of the NMR controversy for hemoglobin in low phosphate, under physiological conditions β His-146 makes a large contribution to the Bohr effect; the best estimates are on the order of 50%.

It has also been suggested that a large number of groups in the protein make significant contributions to the Bohr effect (Russu et al., 1982; Matthew et al., 1979a,b). One such argument is based on NMR studies of histidines in deoxy- and oxyhemoglobin (Russu et al., 1982). By measuring the titration curves for 22 histidines and estimating the pK_a values in Hb and HbO_2, Russu et al. found that the sum of their contributions is "comparable in magnitude" to the Bohr effect observed experimentally. Since individual histidine resonances were not assigned, the measurements do not show which ones are important in the Bohr effect. Further, the results are too crude to provide quantitative information on the Bohr effect; e.g., since not all histidines were observed, it is not possible to be sure that the same histidines were measured in Hb and HbO_2, as would be required to obtain quantitative results.

The involvement of a large number of histidines in Bohr proton release was also suggested by the electrostatic calculations of Gurd and co-workers (Matthew et al., 1979a,b). They used a modified Tanford–Kirkwood–Westheimer model (Kirkwood & Weistheimer, 1938; Tanford & Kirkwood, 1957) and employed the Hb crystal structure to model both Hb and HbO_2. Inconsistencies in the model and the results obtained have been pointed out by Perutz et al. (1980, 1984). Moreover, a more recent electrostatic calculation (Matthew et al., 1985) that used the X-ray structures for both Hb and HbO_2 showed the largest change in pK_a for β His-146 (8.3 in Hb and 6.25 in HbO_2 at an ionic strength of 0.1 M); this contrasts with the earlier calculation, which yielded 8.2 in HbO_2 because the breaking of the salt link to β Asp-94 was neglected. All other histidines were calculated to have much smaller changes between Hb and HbO_2 than β His-146.

It is evident from the above discussion that both the mechanism of the Bohr effect and the interdependence between the Bohr effect and cooperativity require clarification. To provide a more complete framework within which to interpret the experimental data, the original Szabo–Karplus model has been generalized (Lee & Karplus, 1983). An important element of the generalized model (referred to as the SKL model) is the inclusion of two tertiary structures for *each* of the two quaternary structures, in accord with the structural data (Anderson, 1973, 1975) outlined above. In the original SK model all of the salt bridges were tertiary-linked; that is, ligation of a given subunit led to a breaking of the salt bridges originating in that subunit. Further, it was assumed that the six interchain salt bridges were quaternary-linked as well; that is, a change of the quaternary structure from deoxy to oxy led to a breaking of these salt bridges. The two intrasubunit (β chain) salt bridges were assumed to be independent of the quaternary structure. The generalized SKL model introduces the possibility of varying the tertiary and quaternary coupling of all of the salt bridges. It includes the SK model and the pure two-state Monod–Wyman–Changeux model, in which the salt bridges are linked only to the quaternary structure, as special cases.

In the first application of the generalized model (Lee & Karplus, 1983), it was found that the oxygenation binding data of Mills et al. (1976) at a single pH (pH 7.4) were consistent with the SK model, but did not provide sufficient information for the determination of a unique SK or SKL parameter set. An analysis of Bohr data over the range pH 7–9.2 (Antonini et al., 1965) demonstrated that the SK model in its original form could not simultaneously fit both the oxygenation data and the Bohr curves (Lee & Karplus, 1983); Johnson et al. (1984) have found a corresponding result. Introduction of the generalized model (Lee & Karplus, 1983) yielded results in accord with the available data, including the pH dependence. The essential point was the need for the inclusion of pH-independent ligand binding constraints. One approach involved a modification of the SK model to allow different strengths for the salt bridges that are pH dependent and pH independent. Because the Bohr curve depends on only the strengths of the salt bridges with ionizable protons, uncoupling of the pH-independent and pH-dependent salt bridges allows the

Table I: Statistical Parameters of Linear Regression Analyses for K_{41} and K_{44} at Different pH Values

pH	N^a	r^2	std error (estd)	slope (±SE)	log $K_{4i}{}^b$ (±SE)	log $K_{4i}{}^c$ (±SD)
			K_{41}			
6.0–6.2	18	0.970	5×10^{-2}	1.02 (± 0.044)	−1.880 (±0.028)	−1.870 (±0.059)
6.9–7.1	38	0.962	4.7×10^{-2}	1.05 (±0.035)	−1.741 (±0.017)	−1.724 (±0.048)
7.3–7.5	10	0.970	7.0×10^{-2}	0.96 (±0.060)	−1.567 (±0.052)	−1.530 (±0.068)
8.0–8.4	12	0.973	3.8×10^{-2}	1.04 (±0.054)	−1.032 (±0.068)	−1.08 (±0.035)
			K_{44}			
6.5–6.6	15	0.982	2.0×10^{-2}	1.01 (±0.038)	0.057 (±0.072)	0.08 (±0.02)
6.9–7.1	27	0.918	4.4×10^{-2}	0.99 (±0.059)	0.402 (±0.106)	0.39 (±0.048)
7.9–8.1	19	0.910	4.3×10^{-2}	0.95 (±0.072)	0.680 (±0.110)	0.62 (±0.043)
8.5–9.0	10	0.992	2.0×10^{-2}	1.02 (±0.032)	0.665 (±0.040)	0.68 (±0.020)

[a] N is the number of determinations. [b] Values calculated by linear regression analysis; the standard error (SE) is given in parentheses. [c] Mean of individual experimental values calculated from $\log K = \log [\langle y_{O_2} \rangle / (1 - \langle y_{O_2} \rangle)] - \log P$; the standard deviation (SD) is given in parentheses.

oxygenation and Bohr curves to be fitted simultaneously. However, structural data and theoretical results (Gelin et al., 1977, 1983) point to the presence of additional steric constraints imposed by the contacts at the $\alpha_1\beta_2$ and $\alpha_2\beta_1$ interfaces on the ligand affinity in the deoxy quaternary structure. Some recent mutant studies (e.g., Hb San Diego) have suggested that the $\alpha_1\beta_1$ subunit contact may also play a role (Loukopoulos et al., 1986). The presence of such steric constraints in the generalized model, with the simplifying assumption that all salt bridges are of equal strength, also leads to an excellent description of the data (Lee & Karplus, 1983). It is, of course, possible that both types of effects are involved in the reduced coupling between cooperativity and the Bohr effect found in the more recent hemoglobin studies, relative to the original Roughton–Lyster results.

The application of the SKL model to the analysis of the oxygenation and total Bohr proton release curves made clear that additional information was needed for a more complete specification of the cooperative mechanism. Most importantly, a determination of the tertiary versus quaternary coupling of the salt bridges requires more detailed results concerning the proton release as a function of oxygenation. Of particular interest is the proton release at the first ($\Delta H_1{}^+$) and the fourth ($\Delta H_4{}^+$) oxygenation steps since these quantities can best serve to distinguish between the coupling of salt bridges to tertiary and quaternary structural changes. This paper reports some new measurements of $\Delta H_1{}^+$ and $\Delta H_4{}^+$ and utilizes the results to provide a precise determination of the relationship between the Bohr effect and cooperativity in hemoglobin.

The SKL model is reviewed briefly under Theory. Expressions for the Adair constants and for $\Delta H_1{}^+$ and $\Delta H_4{}^+$ in terms of the SKL model are developed. The model expressions for $\Delta H_1{}^+$ and $\Delta H_4{}^+$ are then simplified for the conditions of the experiments to facilitate the data analysis. The results of accurate experimental determinations of $\Delta H_1{}^+$ and $\Delta H_4{}^+$ over a range of pH values (pH 6–9) under controlled solution conditions are given under Experimental Results for $\Delta H_1{}^+$ and $\Delta H_4{}^+$. Under Analysis of Experiments experimentally determined Adair constants at several pH's (Chu et al., 1984) are compared with those calculated with the model parameter sets derived from earlier work (Lee & Karplus, 1983). With the new data for $\Delta H_1{}^+$ and $\Delta H_4{}^+$, a detailed analysis of the tertiary and quaternary coupling of the salt bridges is made. The conclusions that follow from the present treatment are outlined and compared with other models for hemoglobin cooperativity.

Theory

In this section we present a brief description of the generalized model for hemoglobin cooperativity and show how it can be simplified to obtain useful expressions for $\Delta H_1{}^+$ and $\Delta H_4{}^+$.

(A) SKL Model. The tetramer-generating function Ξ for the SKL model (Lee & Karplus, 1983) is given below. We write

$$\Xi(\lambda,\mu) = \Xi_D(\lambda,\mu) + \Xi_O(\lambda,\mu)$$

were D and O refer to the deoxy and oxy quaternary structures, respectively, λ is the oxygen partial pressure, and μ is the hydroxyl ion concentration. The functions $\Xi_D(\lambda,\mu)$ and $\Xi_O(\lambda,\mu)$ have the form

$$\Xi_D(\lambda,\mu) = \frac{Qs^6}{r'^2}\left(1 + \frac{\mu H^\alpha}{S}\right)^2\left(1 + \frac{\mu H^\beta}{S}\right)^2\left[1 + \lambda K_D{}^\alpha r^2\left(\frac{1 + \frac{\mu H^\alpha}{rS}}{1 + \frac{\mu H^\alpha}{S}}\right)\right]^2\left[1 + \lambda K_D{}^\beta r^2\left(\frac{1 + \frac{\mu H^\beta}{rS}}{1 + \frac{\mu H^\beta}{S}}\right)\right]^2$$

$$\Xi_O(\lambda,\mu) = (1 + \mu H^\alpha)^2\left(1 + \frac{\mu H^\beta}{r'S}\right)^2[1 + \lambda K_O{}^\alpha]^2\left[1 + \lambda\frac{K_O{}^\beta}{r'S}\left(\frac{1 + \mu H^\beta}{1 + \frac{\mu H^\beta}{r'S}}\right)\right]^2 \quad (1)$$

Here Q determines the relative stability of the two quaternary states in the absence of ligands and salt bridges, S is the salt-bridge strength of unliganded chains in the deoxy tetramer for ionic interactions of the type $NH_n{}^+ \ldots COO^-$ under a given set of solution conditions, rS is the effective strength of the salt bridges of liganded chains in the deoxy tetramer, $r'S$ is the effective strength of the intra β chain salt bridge in the unliganded oxy tetramer, $K_D{}^\alpha$, $K_D{}^\beta$, $K_O{}^\alpha$, and $K_O{}^\beta$ are the intrinsic ligand affinities for the α and β chains in the two quaternary structures, and H^α and H^β are the hydroxyl binding constants for the Bohr groups in the α and β chains, respectively. H^α and H^β are related to the pK's by $pK^{\alpha(\beta)} = 14 - \log H^{\alpha(\beta)}$. For the purpose of our calculations, only the properties of the tetramer will be considered since dissociation into dimers is not important or is accounted for implicitly in the data used for the analysis. The physical significance of the parameters and the allowed ranges for their values have been discussed previously (Szabo & Karplus, 1972; Lee & Karplus, 1983).

Although the physical assumptions of the SKL model are very different from the concerted two-state behavior that is the essence of the Monod–Wyman–Changeux model (Monod et al., 1965), mathematically the generating function for the SKL model can be written in the MWC form generalized to a tetramer with inequivalent chains; the expression is given by (Ogata & McConnell, 1972; Szabo & Karplus, 1972)

$$\Xi(\lambda) = L(1 + \lambda c^{\alpha}K_R{}^{\alpha})^2(1 + \lambda c^{\beta}K_R{}^{\beta})^2 + (1 + \lambda K_R{}^{\alpha})^2(1 + \lambda K_R{}^{\beta})^2 \quad (2)$$

where L is the allosteric constant, $K_R{}^{\alpha}$ and $K_R{}^{\beta}$ are the ligand affinities of the α and β chains in the oxy state, and $c^{\alpha}K_R{}^{\alpha}$ and $c^{\beta}K_R{}^{\beta}$ are the ligand affinities of the chains in the deoxy state (c^{α},$c^{\beta} < 1$). The SKL model expressions for the MWC parameters are obtained by comparing eq 1 and 2. We have

$$L = \frac{QS^6}{r'^2}\frac{\left(1 + \frac{\mu H^{\alpha}}{S}\right)^2\left(1 + \frac{\mu H^{\beta}}{S}\right)^2}{(1 + \mu H^{\alpha})^2\left(1 + \frac{\mu H^{\beta}}{r'S}\right)^2}$$

$$c^{\alpha} = \frac{K_D{}^{\alpha}}{K_O{}^{\alpha}}r^2\left(\frac{1 + \frac{\mu H^{\alpha}}{rS}}{1 + \frac{\mu H^{\alpha}}{S}}\right)$$

$$c^{\beta} = \frac{K_D{}^{\beta}}{K_O{}^{\beta}}r^2r'S\frac{\left(1 + \frac{\mu H^{\beta}}{r'S}\right)\left(1 + \frac{\mu H^{\beta}}{rS}\right)}{\left(1 + \frac{\mu H^{\beta}}{S}\right)(1 + \mu H^{\beta})}$$

$$K_R{}^{\alpha} = K_O{}^{\alpha} \qquad K_R{}^{\beta} = \frac{K_O{}^{\beta}(1 + \mu H^{\beta})}{r'S\left(1 + \frac{\mu H^{\beta}}{r'S}\right)} \quad (3)$$

The parameter L is always pH dependent, and $K_R{}^{\alpha}$ is always pH independent in the SKL model. For the other parameters, the pH dependence is determined by the values of r or r'. Thus, c^{α} is pH independent when $r = 1$, c^{β} is pH independent when $r = 1$ and $r' = 1/S$, and $K_R{}^{\beta}$ is pH independent when $r' = 1/S$.

Two special cases of the SKL model are the extended SK model ($r = 1/S$, $r' = 1$) and the two-state MWC model ($r = 1$, $r' = 1/S$) (Lee & Karplus, 1983). These represent particular modes of tertiary–quaternary coupling: in the former, salt bridges involving the C-terminus of a given subunit are completely broken when that subunit binds a ligand; in the latter, the salt bridges are linked exclusively to the quaternary structure. In terms of the parameters of eq 3, all but $K_R{}^{\alpha}$ are pH dependent in the extended SK model, while only L is pH dependent in the two-state MWC model. We have assumed, as was done in the original SK model (Szabo & Karplus, 1972), that all intersubunit salt bridges (i.e., except the one internal to the β chain) are broken upon a quaternary transition. Hence, the SKL model does not allow for pure tertiary linkage. The justification of such an assumption must come from an analysis of the structural properties and Bohr effect of hemoglobins whose quaternary structure can be switched in the absence of a change in ligation state. With regard to the unliganded tetramer, the only data available are those for hemoglobins modified at the C-termini [des-Arg-141α, NES-des-Arg-141α, des-(Arg-141α,Tyr-140α), des-(Arg-141α,His-146β) (Kilmartin et al., 1975)]. These exist primarily in the oxy quaternary structure even when unliganded and can be switched to the deoxy quaternary structure by inositol hexaphosphate (IHP). Unfortunately, the modifications necessary to lock the molecule in one or the other quaternary structure involve the salt bridges whose properties we wish to determine. With regard to the liganded case, the X-ray studies of systems such as fluoromet-hemoglobin (Fermi & Perutz, 1977), which can undergo the oxy → deoxy quaternary transition upon addition of IHP, suggest that the intersubunit salt bridges form during this transition. Thus, in the absence of specific contrary data and guided by the structures of the liganded oxy tetramer and unliganded deoxy tetramer (Perutz, 1970a,b; Shaanan, 1983; Fermi, 1984), we assume all intersubunit salt bridges to be essentially coupled to the quaternary structure.

(*B*) *Adair Constants in the SKL Model.* The generating function corresponding to the Adair equation (Adair, 1925) is

$$\Xi(\lambda) = 1 + \lambda K_{41} + \lambda^2K_{41}K_{42} + \lambda^3K_{41}K_{42}K_{43} + \lambda^4K_{41}K_{42}K_{43}K_{44} \quad (4a)$$

where K_{4i} ($i = 1$–4) are the tetramer equilibrium constants uncorrected for statistical factor describing the reaction

$$Hb(O_2)_{i-1} + O_2 \rightleftarrows Hb(O_2)_i$$

that is

$$K_{4i} = \frac{[Hb(O_2)_i]}{[O_2][Hb(O_2)_{i-1}]} \quad (4b)$$

For simplicity of writing, the corresponding SKL model expressions for K_{4i} are obtained in terms of the parameters of the general MWC equation (eq 2). After expanding, collecting terms in λ, and factoring out $L + 1$, we have, using eq 4b

$$K_{41} = 2[L(c^{\alpha}K_R{}^{\alpha} + c^{\beta}K_R{}^{\beta}) + (K_R{}^{\alpha} + K_R{}^{\beta})]/(L + 1)$$

$$K_{42} = \{L[(c^{\alpha}K_R{}^{\alpha})^2 + 4(c^{\alpha}K_R{}^{\alpha})(c^{\beta}K_R{}^{\beta}) + (c^{\beta}K_R{}^{\beta})^2] + (K_R{}^{\alpha 2} + 4K_R{}^{\alpha}K_R{}^{\beta} + K_R{}^{\beta 2})\}/\{2[L(c^{\alpha}K_R{}^{\alpha} + c^{\beta}K_R{}^{\beta}) + (K_R{}^{\alpha} + K_R{}^{\beta})]\}$$

$$K_{43} = 2[Lc^{\alpha}K_R{}^{\alpha}c^{\beta}K_R{}^{\beta}(c^{\alpha}K_R{}^{\alpha} + c^{\beta}K_R{}^{\beta}) + K_R{}^{\alpha}K_R{}^{\beta}(K_R{}^{\alpha} + K_R{}^{\beta})]/\{L[(c^{\alpha}K_R{}^{\alpha})^2 + 4(c^{\alpha}K_R{}^{\alpha})(c^{\beta}K_R{}^{\beta}) + (c^{\beta}K_R{}^{\beta})^2] + (K_R{}^{\alpha 2} + 4K_R{}^{\alpha}K_R{}^{\beta} + K_R{}^{\beta 2})\}$$

$$K_{44} = \tfrac{1}{2}[L(c^{\alpha}K_R{}^{\alpha}c^{\beta}K_R{}^{\beta})^2 + (K_R{}^{\alpha}K_R{}^{\beta})^2]/[Lc^{\alpha}K_R{}^{\alpha}c^{\beta}K_R{}^{\beta}(c^{\alpha}K_R{}^{\alpha} + c^{\beta}K_R{}^{\beta}) + K_R{}^{\alpha}K_R{}^{\beta}(K_R{}^{\alpha} + K_R{}^{\beta})] \quad (5)$$

where the MWC parameters L, c^{α}, c^{β}, $K_R{}^{\alpha}$, and $K_R{}^{\beta}$ are given by eq 3.

All of the Adair constants in eq 5 depend on r and r', but the ones most accessible to experimental determination are K_{41} and K_{44}. This can be seen by first writing down the Adair expression for the fractional saturation of the tetramer with oxygen, $\langle y_{O_2}\rangle$ (Wyman, 1964)

$$\langle y_{O_2}\rangle = \frac{\partial \ln \Xi}{4\partial \ln \lambda} = (\lambda K_{41}' + 3\lambda^2K_{41}'K_{42}' + 3\lambda^3K_{41}'K_{42}'K_{43}' + \lambda^4K_{41}'K_{42}'K_{43}'K_{44}')/(1 + 4\lambda K_{41}' + 6\lambda^2K_{41}'K_{42}' + 4\lambda^3K_{41}'K_{42}'K_{43}' + \lambda^4K_{41}'K_{42}'K_{43}'K_{44}') \quad (4c)$$

where K_{4i}' are the sequential Adair constants corrected for statistical factors. They are related to K_{4i} by the equation

$$K_{4i} = \frac{4 - i + 1}{i}K_{4i}' \quad (4d)$$

If the fractional saturation data are plotted as ln $[\langle y_{O_2}\rangle/(1 - \langle y_{O_2}\rangle)]$ on the y axis and ln λ on the x axis in a Hill plot, the two asymptotic limits are given by

$$\lambda \ll 1 \qquad \ln \frac{\langle y_{O_2} \rangle}{1 - \langle y_{O_2} \rangle} = \ln K_{41}' + \ln \lambda \qquad (4e)$$

$$\lambda \gg 1 \qquad \ln \frac{\langle y_{O_2} \rangle}{1 - \langle y_{O_2} \rangle} = \ln K_{44}' + \ln \lambda$$

Thus, the x-axis intercept for a tangent to the straight line portion of the Hill plot when $\lambda \ll 1$ gives $-\ln K_{41}'$; the x-axis intercept when $\lambda \gg 1$ gives $-\ln K_{44}'$. If measurements of $\langle y_{O_2} \rangle$ are taken well into the asymptotic ranges, the first and last Adair constants are easily determined without the need for extensive data fitting.

(C) Proton Release at the First (ΔH_1^+) and Last (ΔH_4^+) Oxygenation Steps. To determine the salt-bridge coupling parameters r and r', we utilize ΔH_1^+ and ΔH_4^+, the first derivatives of K_{41} and K_{44} with respect to pH. These quantities can conveniently be separated into contributions whose importance depends on the choice of r and r'. Thus, the model expressions for ΔH_1^+ and ΔH_4^+ can be simplified in the appropriate ranges of solution conditions and utilized directly for data analysis. This contrasts with the expressions for K_{41}' and K_{44}' themselves, which must be used in their exact form and are more difficult to employ in extracting parameter values from the data.

(1) SKL Expression for ΔH_1^+. Exact. The proton release at the first step (ΔH_1^+) is used to evaluate the parameters that determine the effect of ligation on salt bridges in the deoxy tetramer. To do so, we write the SKL expression for ΔH_1^+ by means of the Wyman relationship (1964)

$$\left[\frac{\partial \log K_{41}'}{\partial \mathrm{pH}}\right]_\lambda = 4[\langle y \rangle_H^0 - \langle y \rangle_H^1] \qquad (6a)$$

where $\langle y \rangle_H^0$ and $\langle y \rangle_H^1$ are the number of protons bound per Bohr group for the unliganded and singly liganded tetramers, respectively. Thus, the proton release (defined as positive if $\langle y \rangle_H^1 < \langle y \rangle_H^0$) is given by

$$\Delta H_1^+ = \left[\frac{\partial \log K_{41}'}{\partial \mathrm{pH}}\right]_\lambda \qquad (6b)$$

We can rewrite ΔH_1^+ in the form (Lee, 1984)

$$\Delta H_1^+ = \frac{L_1}{L_1 + 1}\left[\frac{\partial \log K_{41}^{\mathrm{D}}}{\partial \mathrm{pH}}\right]_\lambda + \frac{L_1 - L}{(L_1 + 1)(L + 1)}\left[\frac{\partial \log L}{\partial \mathrm{pH}}\right]_\lambda + \frac{1}{L_1 + 1}\left[\frac{\partial \log K_{41}^{\mathrm{O}}}{\partial \mathrm{pH}}\right]_\lambda \qquad (7a)$$

where L is given by eq 3 and

$$K_{41}^{\mathrm{D}} = \frac{[\mathrm{HbO_2}]_{\mathrm{D}}}{[\mathrm{O_2}][\mathrm{Hb}]_{\mathrm{D}}} = 2r^2\left[K_{\mathrm{D}}^{\alpha}\left(\frac{1 + \frac{\mu H^\alpha}{rS}}{1 + \frac{\mu H^\alpha}{S}}\right) + K_{\mathrm{D}}^{\beta}\left(\frac{1 + \frac{\mu H^\beta}{rS}}{1 + \frac{\mu H^\beta}{S}}\right)\right]$$

$$K_{41}^{\mathrm{O}} = \frac{[\mathrm{Hb(O_2)}]_{\mathrm{O}}}{[\mathrm{Hb}]_{\mathrm{O}}[\mathrm{O_2}]} = 2\left[K_{\mathrm{O}}^{\alpha} + K_{\mathrm{O}}^{\beta}\left(\frac{1 + \mu H^\beta}{r'S\left(1 + \frac{\mu H^\beta}{r'S}\right)}\right)\right]$$

and

$$L_1 = L(K_{41}^{\mathrm{D}}/K_{41}^{\mathrm{O}})$$

The derivatives with respect to pH are given by

$$\left[\frac{\partial \log K_{41}^{\mathrm{D}}}{\partial \mathrm{pH}}\right]_\lambda = \frac{1 - r}{rS}\left[\frac{\mu H^\alpha}{\left(1 + \frac{\mu H^\alpha}{S}\right)^2} + \frac{K_{\mathrm{D}}^{\beta}\mu H^\beta}{K_{\mathrm{D}}^{\alpha}\left(1 + \frac{\mu H^\beta}{S}\right)^2}\right] \times \left[\frac{1 + \frac{\mu H^\alpha}{rS}}{1 + \frac{\mu H^\alpha}{S}} + \frac{K_{\mathrm{D}}^{\beta}\left(1 + \frac{\mu H^\beta}{rS}\right)}{K_{\mathrm{D}}^{\alpha}\left(1 + \frac{\mu H^\beta}{S}\right)}\right]^{-1}$$

$$\left[\frac{\partial \log L}{\partial \mathrm{pH}}\right]_\lambda = \frac{2\mu H^\beta(r' - 1)}{\left(1 + \frac{\mu H^\beta}{S}\right)\left(1 + \frac{\mu H^\beta}{r'S}\right)r'S} - \frac{2\mu H^\alpha(S - 1)}{\left(1 + \frac{\mu H^\alpha}{S}\right)(1 + \mu H^\alpha)S}$$

$$\left[\frac{\partial \log K_{41}^{\mathrm{O}}}{\partial \mathrm{pH}}\right]_\lambda = \frac{\mu H^\beta(r'S - 1)}{\left[r'S\left(1 + \frac{\mu H^\beta}{r'S}\right)\right]^2} \times \frac{K_{\mathrm{O}}^{\mathrm{B}}}{\left\{K_{\mathrm{O}}^{\alpha} + K_{\mathrm{O}}^{\beta}\left[\frac{1 + \mu H^\beta}{r'S\left(1 + \frac{\mu H^\beta}{r'S}\right)}\right]\right\}} \qquad (7b)$$

The first term in eq 7a describes the protons released when oxygen binds to unliganded hemoglobin in the deoxy quaternary state. The second term arises from the titration of the allosteric constant (L) since oxygen binding results in a shift in the ratio of deoxy-state to oxy-state tetramers. The third term is due to proton release when oxygen binds to unliganded tetramers with the oxy quaternary structure.

Approximate. To estimate r from experimental data, it is useful to simplify eq 7a and 7b, which depend on all of the parameters of the model. Since we are concerned with the proton release on binding the first oxygen, terms involving r', K_{O}^{α}, and K_{O}^{β}, which describe the properties of the oxy tetramer, are expected to be insignificant under the solution conditions used for the experiments. We assume that L_1, the relative concentration of singly liganded species in the deoxy quaternary state, is much greater than unity. The pH range over which this approximation is valid is considered under Analysis of Experiments. The first term in eq 7a is the primary contribution to ΔH_1^+ for the extended SK model but is zero for the MWC limit ($r = 1$). The second term in eq 7a is negligible in the extended SK model ($r' = 1$) because the pH at which the assumption $L_1 \gg 1$ breaks down is also the pH at which very few unliganded α chains remain to contribute to the proton release during the quaternary transition (i.e.,

Table II: Summary of Parameter Sets Used in the Analysis of ΔH_1^+ and ΔH_4^+[a]

set	model	pK^α	pK^β	$-RT \ln Q$	$-RT \ln S$	$-RT \ln rS$	$-RT \ln r'S$	$-RT \ln K_D^\alpha$	$-RT \ln K_D^\beta$	$-RT \ln K_O^\alpha$	$-RT \ln K_O^\beta$
A[b]	extended SK	7.5	6.2	5.94	−2.15	0	−2.15	−8.33	−8.82	−8.72	−8.59
	MWC	7.5	6.2	6.15	−2.08	−2.08	0	−5.43	−5.43	−8.50	−8.50
B[b]	extended SK	7.5	7.0	3.88	−1.75	0	−1.75	−7.35	−8.68	−8.57	−8.86
	MWC	7.5	7.0	4.32	−1.68	−1.68	0	−5.43	−5.43	−8.50	−8.50
C[c]	extended SK	6.96	6.75	0.99	−1.69	0	−1.69	−7.29	−8.28	−8.94	−9.38
	MWC	6.96	6.75	2.59	−1.69	−1.69	0	−4.65	−5.77	−8.96	−8.52
D[d]	extended SK	6.96	6.51	1.06	−1.69	−0.16	−1.69	−8.26	−6.75	−8.80	−9.28

[a] All energies in kilocalories per mole. [b] Fit to Roughton–Lyster data at pH 7 and 9.1 (Lee, 1984). [c] Fit to data generated with Adair constants reported by Mills et al. (1976) and to Bohr data (Antonini et al., 1964); see Lee and Karplus (1983). [d] Fit to data generated with Adair constants reported by Mills et al. (1976) and to Bohr data (Antonini et al., 1964); see Lee (1984).

$\partial \log L/\partial$pH is small). For the MWC model, the importance of this term depends on the precise choice of parameters (see Analysis of Experiments). Finally, the last term in eq 7a can be safely neglected for any model because $(L_1 + 1)^{-1}$ is negligible when $r' \approx 1$ and because $\partial \log K_{41}^{O}/\partial$pH is zero when $r' \approx 1/S$.

To obtain the most useful approximations, three regimes of r and r' must be considered: (a) $r \geq 1/S$ and $r' \approx 1$ (extended SK limit); (b) $r \approx 1$ and $r' \geq 1/S$ (MWC limit); and (c) the intermediate values of r and r' ($1/S \leq r, r' < 1$).

Extended SK Limit. For $r \geq 1/S$ and $r' \approx 1$ with $L \gg 1$ and $L_1 \gg 1$, we have

$$\Delta H_1^+ \cong \frac{1-r}{rS}\left[\frac{\mu H^\alpha}{\left(1+\frac{\mu H^\alpha}{S}\right)^2} + \frac{\mu H^\beta}{\left(1+\frac{\mu H^\beta}{S}\right)^2}\frac{K_D^\beta}{K_D^\alpha}\right] \times \left[\frac{1+\frac{\mu H^\alpha}{rS}}{1+\frac{\mu H^\alpha}{S}} + \left(\frac{1+\frac{\mu H^\beta}{rS}}{1+\frac{\mu H^\beta}{S}}\right)\frac{K_D^\beta}{K_D^\alpha}\right]^{-1} \quad (8a)$$

In the above equation, the parameters involved are r, S, K_D^β/K_D^α, pK^α, and pK^β. We note that it is the ratio of ligand affinities of the α and β chains in the deoxy state (i.e., K_D^β/K_D^α) that determines ΔH_1^+.

MWC Limit. For $r \approx 1$ and $r' \geq 1/S$ with $L \gg 1$, we have

$$\Delta H_1^+ \cong \frac{1}{L_1+1}\left[2\frac{S-1}{S}\frac{\mu H^\alpha}{(1+\mu H^\alpha)\left(1+\frac{\mu H^\alpha}{S}\right)} - 2\frac{r'-1}{r'S}\frac{\mu H^\beta}{(1+\mu H^\beta)\left(1+\frac{\mu H^\beta}{S}\right)}\right] \quad (8b)$$

This equation is more complicated than eq 8a because of the presence of L_1, which is a function of all of the parameters in the model. However, when $r \approx 1$, L_1 can be simplified and is accurately approximated by

$$L_1 \approx \frac{QS^6}{r'^2}\frac{\left(1+\frac{\mu H^\alpha}{S}\right)^2}{(1+\mu H^\alpha)^2}\frac{\left(1+\frac{\mu H^\beta}{S}\right)^2}{(1+\mu H^\beta)^2}\frac{K_D^\alpha + K_D^\beta}{K_O^\alpha + K_O^\beta}$$

so that Q and the ratio of the intrinsic affinities of the deoxy and oxy tetramers appear as a scaling factor. When $r = 1$ and $r' = 1/S$, eq 8b gives the total proton release [eq 2 of Lee and Karplus (1983)]. In this case, the number of Bohr protons released at the first step depends on just the shift in the quaternary equilibrium upon binding the first oxygen. From eq 8b, we see that ΔH_1^+ is significant only if pK^α and pK^β are in the alkaline range (see Analysis of Experiments). This is because at neutral pH the term containing L_1 is negligible, while at alkaline pH the second term is negligible unless the Bohr curve peaks in this region.

Intermediate Region. Assuming that $L \gg 1$, eq 7a becomes

$$\Delta H_1^+ = \frac{L_1}{L_1+1}\left[\frac{\partial \log K_{41}^{D}}{\partial \text{pH}}\right]_\lambda - \frac{1}{L_1+1}\left[\frac{\partial \log L}{\partial \text{pH}}\right]_\lambda + \frac{1}{L_1+1}\frac{\partial \log K_{41}^{O}}{\partial \text{pH}} \quad (8c)$$

(2) SKL Expression for ΔH_4^+. Exact. We write the SKL expression for ΔH_4^+ using the Wyman relationship (Wyman, 1964)

$$\Delta H_4^+ = \left[\frac{\partial \log K_{44}'}{\partial \text{pH}}\right]_\lambda \quad (9)$$

By following a development analogous to that described for K_{41} (Lee, 1984), we have

$$\Delta H_4^+ = \frac{L_3}{L_3+1}\left[\frac{\partial \log K_{44}^{O}}{\partial \text{pH}}\right]_\lambda + \frac{L_4 - L_3}{(L_4+1)(L_3+1)}\left[\frac{\partial \log L_4}{\partial \text{pH}}\right]_\lambda + \frac{1}{L_3+1}\left[\frac{\partial \log K_{44}^{D}}{\partial \text{pH}}\right]_\lambda \quad (10a)$$

where

$$L_3 = L_4\frac{K_{44}^{D}}{K_{44}^{O}}$$

$$L_4 = \frac{[\text{Hb}(\text{O}_2)_4]_O}{[\text{Hb}(\text{O}_2)_4]_D} = \left[\frac{K_O^\alpha K_O^\beta}{K_D^\alpha K_D^\beta}\right]^2 \frac{1}{Q(rS)^8}\left[\frac{(1+\mu H^\alpha)(1+\mu H^\beta)}{\left(1+\frac{\mu H^\alpha}{rS}\right)\left(1+\frac{\mu H^\beta}{rS}\right)}\right]^2$$

$$K_{44}^{O} = \frac{[\text{Hb}(\text{O}_2)_4]_O}{[\text{O}_2][\text{Hb}(\text{O}_2)_3]_O} = \frac{K_O^\alpha K_O^\beta(1+\mu H^\beta)}{r'S\left(1+\frac{\mu H^\beta}{r'S}\right)}\left[K_O^\alpha + \frac{K_O^\beta(1+\mu H^\beta)}{r'S\left(1+\frac{\mu H^\beta}{r'S}\right)}\right]^{-1}$$

and

$$K_{44}^{D} = \frac{[Hb(O_2)_4]_D}{[O_2][Hb(O_2)_3]_D} = \frac{K_D^{\alpha}K_D^{\beta}\left(1+\frac{\mu H^{\alpha}}{rS}\right)\left(1+\frac{\mu H^{\beta}}{rS}\right)}{\left(1+\frac{\mu H^{\alpha}}{S}\right)\left(1+\frac{\mu H^{\beta}}{S}\right)} \times \left[K_D^{\alpha}\left(\frac{1+\frac{\mu H^{\alpha}}{rS}}{1+\frac{\mu H^{\alpha}}{S}}\right) + K_D^{\beta}\left(\frac{1+\frac{\mu H^{\beta}}{rS}}{1+\frac{\mu H^{\beta}}{S}}\right)\right]^{-1}$$

The derivatives of these terms required for eq 10a are

$$\left[\frac{\partial \log K_{44}^{O}}{\partial pH}\right]_{\lambda} = \frac{\mu H^{\beta}}{(1+\mu H^{\beta})\left(1+\frac{\mu H^{\beta}}{r'S}\right)} \frac{r'S-1}{r'S} \times \frac{1}{1+\frac{K_O^{\beta}}{K_O^{\alpha}}\frac{1+\mu H^{\beta}}{r'S\left(1+\frac{\mu H^{\beta}}{r'S}\right)}}$$

$$\left[\frac{\partial \log L_4}{\partial pH}\right]_{\lambda} = \frac{2(rS-1)}{rS}\left[\frac{\mu H^{\alpha}}{(1+\mu H^{\alpha})\left(1+\frac{\mu H^{\alpha}}{rS}\right)} + \frac{\mu H^{\beta}}{(1+\mu H^{\beta})\left(1+\frac{\mu H^{\beta}}{rS}\right)}\right]$$

$$\left[\frac{\partial \log K_{44}^{D}}{\partial pH}\right]_{\lambda} = \frac{1-r}{rS}\left[\frac{\mu H^{\alpha}}{\left(1+\frac{\mu H^{\alpha}}{S}\right)\left(1+\frac{\mu H^{\alpha}}{rS}\right)} + \frac{\mu H^{\beta}}{\left(1+\frac{\mu H^{\beta}}{S}\right)\left(1+\frac{\mu H^{\beta}}{rS}\right)}\right] - \frac{1-r}{rS}\left[\frac{\mu H^{\alpha}}{\left(1+\frac{\mu H^{\alpha}}{S}\right)^2} + \frac{K_D^{\beta}\mu H^{\beta}}{K_D^{\alpha}\left(1+\frac{\mu H^{\beta}}{S}\right)^2}\right] \times \left[\frac{1+\frac{\mu H^{\alpha}}{rS}}{1+\frac{\mu H^{\alpha}}{S}} + \frac{\left(1+\frac{\mu H^{\beta}}{rS}\right)K_D^{\beta}}{\left(1+\frac{\mu H^{\beta}}{S}\right)K_D^{\alpha}}\right]^{-1} \quad (10b)$$

The first and third terms in eq 10a are the proton release brought about by the oxygenation of triply liganded tetramers in the oxy and deoxy quaternary state, respectively, while the second term is the proton release arising from the shift in the ratio of fully liganded tetramers in the oxy to deoxy quaternary state.

Approximate. To obtain an understanding of how the different parameters influence ΔH_4^+, eq 10a and 10b must be simplified. From eq 10b we see that the first term in eq 10a drops out when $r' = 1/S$; the second term can be neglected if (a) $r = 1/S$ so that $\partial \log L_4/\partial pH = 0$ and/or (b) $L_3 \gg 1$ and $L_4 \gg 1$ so that $(L_4 - L_3)/[(L_4 + 1)(L_3 + 1)] \cong 0$. The pH ranges over which the assumptions $L_3 \gg 1$ and $L_4 \gg 1$ should be valid are discussed under Analysis of Experiments. We consider three regimes: (a) the extended SK limit with $r \approx 1/S$ and $r' \approx 1$, (b) the MWC limit with $r \approx 1$ and $r' \approx 1/S$, and (c) the intermediate range of r and r' ($1/S \leq r, r' < 1$).

Extended SK Limit. For $r \approx 1/S$, $\partial \log L_4/\partial pH$ is approximately zero. In addition, we assume that $L_3 \gg 1$ and $L_4 \gg 1$. Then we have

$$\Delta H_4^+ \cong \left[\frac{\partial \log K_{44}^{O}}{\partial pH}\right]_{\lambda} \quad (11a)$$

The parameters involved are r', S, K_O^{β}/K_O^{α}, and pK^{β}, as can be seen from eq 10b. The characteristics of the pH profile are defined by $(\Delta H_4^+)_{max}$ and pH_{max}, where pH_{max} is obtained by setting $\partial \Delta H_4^+/\partial pH = 0$ and $(\Delta H_4^+)_{max}$ is the value of ΔH_4^+ at this pH. We find

$$pH_{max} = pK^{\beta} + \tfrac{1}{2} \log \frac{r'S + K_O^{\beta}/K_O^{\alpha}}{1 + K_O^{\beta}/K_O^{\alpha}} \quad (11b)$$

Substituting this value for μH^{β} into the expression for $\partial \log K_{44}^{O}/\partial pH$, we obtain

$$(\Delta H_4^+)_{max} = \frac{r'S - 1}{[(1 + K_O^{\beta}/K_O^{\alpha})^{1/2} + (r'S + K_O^{\beta}/K_O^{\alpha})^{1/2}]^2} \quad (11c)$$

Equation 11b shows that the observed pH_{max} provides an upper limit of pK^{β}. In addition, since there are four parameters and only two experimental variables [pH_{max} and $(\Delta H_4^+)_{max}$], the proton release curve cannot yield unique values for r' unless at least two of the other parameters have been determined independently.

MWC Limit. For $r \approx 1$, $\partial \log K_{44}^{D}/\partial pH$ is approximately zero, and for $r' \approx 1/S$, $\partial \log K_{44}^{O}/\partial pH$ is approximately zero. If we assume that $L_4 \gg 1$, eq 10a reduces to

$$\Delta H_4^+ = \frac{1}{L_3 + 1}\left[\frac{\partial \log L_4}{\partial pH}\right]_{\lambda} \quad (12)$$

In the MWC limit and for the parameter sets in use, L_3 is of the order of unity in the pH range of interest (see Analysis of Experiments) and cannot be neglected in eq 12. Because of this dependence on L_3, the pH behavior of K_{44}' for the MWC model is strongly coupled to the cooperativity of the system. This is seen most clearly by considering the case for equivalent chains, in which $L_3 = [Lc^3]^{-1}$, where c is the ratio of the deoxy and oxy state affinities. We note that L_3 decreases with an increase in either L or c. When L increases, the cooperativity of the system, as measured by n, the Hill constant, can increase, decrease, or remain unchanged, depending on where the system is initially located on the n vs log L bell-shaped curve (Edelstein, 1971; Szabo & Karplus, 1972). When c increases, the cooperativity always decreases, and since L_3 varies as $1/c^3$, ΔH_4^+ is very sensitive to variations in c. Hence the more cooperative the system is as a function of c^3,

the smaller ΔH_4^+ is expected to be.

Intermediate Region. For intermediate values of r and r', we assume that $L_4 \gg 1$ in eq 10a to obtain

$$\Delta H_4^+ = \frac{L_3}{L_3 + 1}\left[\frac{\partial \log K_{44}^O}{\partial \mathrm{pH}}\right]_\lambda - \frac{1}{L_3 + 1}\left[\frac{\partial \log L_4}{\partial \mathrm{pH}}\right]_\lambda + \frac{1}{L_3 + 1}\left[\frac{\partial \log K_{44}^D}{\partial \mathrm{pH}}\right]_\lambda \quad (13)$$

Experimental Results for ΔH_1^+ and ΔH_4^+

Hemoglobin was prepared from hemolysates of nonsmoking blood donors by using DEAE-Sephadex column chromatography and a linear pH gradient of 50 mM tris(hydroxymethyl)aminomethane hydrochloride (Tris-HCl) buffer from pH 7.9 to 6.9. The purity of the isolated HbA ($\alpha_2\beta_2$) was verified by isoelectrofocusing, which revealed a single band migrating at pH 6.95. After isolation, HbA was freed of the remaining small anions by passing the solution on a mixed bed ion-exchange resin (Bio-Rad AG 50 1-X8) concentrated under nitrogen gas pressure in a Diaflo Amicon cell and then kept frozen in small droplets in liquid nitrogen until use. To check the amount of methemoglobin present, the sample was thawed at room temperature, and the visible electronic absorption spectrum of the oxygenated diluted stock solution was recorded with a Cary 219 spectrophotometer. From the ratio $A_{576.5\mathrm{nm}}/A_{500\mathrm{nm}}$ at pH 7.0, 25 °C (Kilmartin et al., 1978), less than 1% methemoglobin was present.

(*A*) *Oxygen Binding Measurements.* Oxygen binding measurements at equilibrium were carried out as described (Poyart et al., 1978, 1980). The stock solution of pure HbA (15–18 mM heme) was diluted to 0.7–0.8 mM on a heme basis in the desired buffered medium in 100-mL glass tonometers sealed onto 0.2-cm light path optical cuvettes. Under these conditions the difference in absorbance at 576.5 nm for 1% oxygen saturation is 0.01 unit, well over the precision of absorbance readings with the Cary 219 spectrophotometer. The Hb solutions were first equilibrated with pure oxygen and exposed for 30 min under intense light (250 W × 2 bulbs) in an ice–water bath under gentle agitation in order to remove any trace of carbon monoxide that might have been bound to the Hb during exposure to room air. The Hb solutions were completely deoxygenated at 25 °C in the same glass tonometer under humidified pure argon (Van Assendelft, 1970). Deoxygenation was considered to be complete when the ratio of absorbances at 554.5–540 nm was >1.27. The ratio is indicative of the absence of contaminating HbCO (Kilmartin et al., 1978). Successive oxygenation was achieved by adding precise amounts of oxygen in argon mixtures with a calibrated Hamilton gas-tight syringe through a rubber-capped side hole. The volume of the tonometers had been determined previously by weight. The oxygen partial pressure, $P_{O_2} = \lambda$, was calculated from the volume of oxygen added and the volume of the gas phase. Percentages of liganded Hb were estimated from the relative absorbances at 576.5 and 560 nm. The absorbance at 568.3 nm, an isosbestic point, was also recorded at each step. A variation of less than 2% in each measurement during the 2-h period of the experiment was considered as negligible in terms of methemoglobin formation or protein denaturation. After each addition of the oxygen–argon gas mixture, the solution was equilibrated by gentle manual agitation in a thermostated water bath at 25 °C for at least 10–15 min. After 5 min of equilibration, the same volume of gas was withdrawn from the tonometer with the Hamilton syringe so as to keep the pressure constant inside the tonometer.

The temperature was kept constant at 25 ± 0.1 °C in the thermostated cuvette holder and checked with a thermoprobe in the reference cuvette. At the end of the experiment, the Hb solution was equilibrated with pure humidified oxygen to determine the absorbance of the fully liganded Hb at the two wavelengths and to check for methemoglobin formation during the experiment. All experiments in which more than 3% oxidation had occurred were discarded.

Buffers. The media used in this study were made with doubly distilled water, 50 mM 2-[bis(2-hydroxyethyl)-amino]-2-(hydroxymethyl)-1,3-propanediol (Bis-Tris), or 50 mM Tris for pH values greater than 7.5 and 0.1 M NaCl adjusted to the desired pH value with HCl or NaOH. The amount of chloride added in pH adjustments was taken into account in the final chloride concentration. All chemicals used were of analytical grade.

Gas. The gases were provided by Compagnie Française des Produits Oxygénés (Nanterre, France). Oxygen and argon were of the purest grade available (N_{45} and N_{60}, respectively). For the determination of oxygen binding at very low P_{O_2} values, a mixture of 1.04 ± 0.03% oxygen N_{45} in argon was used.

(*B*) *Determination of K_{41}.* Oxygen binding experiments at oxygen saturation values $\langle y_{O_2}\rangle$ below 0.015 [$\log [\langle y_{O_2}\rangle/(1 - \langle y_{O_2}\rangle)] \leq -1.75$] were carried out according to the general procedure described above and the 1.04% oxygen in argon gas mixture. Catalase (20 μg/mL) was the only reducing agent added to the Hb solutions in order to avoid any possible influence of glucose 6-phosphate, which is part of the complete Hayashi reducing system (Hayashi et al., 1973). For each individual experiment where only three to four data points were collected below $\langle y_{O_2}\rangle$ <0.015, $\log K_{41}$ was estimated as a first approximation from the relation $\log [\langle y_{O_2}\rangle/(1 - \langle y_{O_2}\rangle)] - \log P = \log K$, assuming a slope of unity in this range of saturation values. For the whole set of experiments at each individual pH value, $\log K_{41}$ was obtained by linear regression analysis of at least 10 data points. The mean values obtained by the two methods are given in the last two columns of Table I.

(*C*) *Determination of P_{50} and n_{50}.* The P_{50} and n_{50} values representing the partial pressure of O_2 and the Hill coefficient values at half-saturation were measured in the same experiments following the determination of K_{41}. Aliquots of pure oxygen were added to the tonometer in order to obtain saturation values in the middle portion of the oxygen binding curve. Four to six points were measured for $\langle y_{O_2}\rangle$ between 0.2 and 0.8. $\log P_{50}$ and n_{50} were then calculated by linear regression analysis with the Hill equation.

(*D*) *Determination of K_{44}.* Two different techniques were used. One was similar to the method described above for the determination of K_{41} in 0.6–0.8 mM heme solutions at 25 °C except that progressive deoxygenation was carried out on fully oxygenated samples. The hemoglobin solutions were equilibrated in the vessels at decreasing P_{O_2} values for 10–15 min. P_{O_2} was varied by mixing fractions of pure oxygen with increasing fractions of pure argon with a precisely calibrated gas mixing pump (M 100A, Wosthoff, Bochum, FRG). The accuracy of the pump had been checked before the experiments by the manufacturer and also in our laboratory with an oxygen analyzer (Servomex, Crowborough, Sussex, England). In these experiments the enzymatic reducing system (Hayashi et al., 1973) was added to the solutions. Optical readings were made as described above, and $\log K_{44}$ was calculated by the same methods used for K_{41} for saturation values corresponding to $\langle y_{O_2}\rangle \geq 0.985$. The mean values are given in the last two columns of Table I. After these points were recorded, lower

P_{O_2} values were studied to estimate P_{50}. No significant differences were observed between these P_{50} values and those measured after the K_{41} determinations.

Since 3–4% dimers at the maximum are present in fully oxygenated solutions at a heme concentration of 0.7–0.8 mM, assuming a value of the tetramer to dimer dissociation constant of 10^{-6} M, the effect of protein concentration on the values of K_{44} was determined. Fractional saturation changes upon stepwise deoxygenation were measured in concentrated HbA solutions (7.15 and 16 mM heme). These measurements were carried out with the thin-layer optical cell described by Dolman and Gill (1978). In these experiments, the concentrated Hb solutions were dialyzed overnight against the buffer mixture at 4 °C, concentrated under vacuum, and analyzed after addition of the enzymatic reducing system. It will be shown under Results that within experimental accuracy no significant difference was observed in the K_{44} values measured at 0.7 mM and 7 or 16 mM heme.

It has not been possible to obtain values of K_{44} for pH values below 6.5. Under the conditions used at acidic pH, some wavelength dependence and scattered absorbance values were present at the isosbestic point. This precludes accurate evaluation of K_{44}.

(*E*) *Results.* Parts a–c of Figure 1 show the experimental values of log K_{41}, log P_{50}, and log K_{44} as a function of pH. Parts a and b of Figure 2 show examples of regression lines calculated from the experimental data points at varying pH values for log K_{41} and log K_{44}. Parts c and d of Figure 2 illustrate the distribution of the standard residuals for these series; they demonstrate normal distributions of the experimental errors. Table I gives the statistical parameters of the linear regression analyses for these determinations. Values for log K_{41} are well within the range of values published by others under identical conditions of pH, ionic strength, and temperature in the absence of phosphate (Kilmartin et al., 1978; Imai, 1982). Great care was taken in these experiments to avoid the presence of HbCO and met-Hb, the two major contaminating species that can lead to an artificial decrease of K_{41} (Kilmartin et al., 1978). As demonstrated by Kilmartin et al. and confirmed by us (unpublished results), Hb concentration has no influence on the K_{41} values beyond 100 μM in heme. The present results show also (Figure 1c) that the values for K_{44} were not significantly different whether determined in solutions of 0.8, 7.2, or 16 mM heme. Whereas the values for K_{41} in the entire pH range studied and for K_{44} from pH 7 to 9 are well-behaved, the values for K_{44} below pH 6.7 are more uncertain. This can be explained neither by the met-Hb content (always lower than 3%) nor by an increasing amount of liganded low-affinity deoxy-state tetramers at low pH. At low pH the mean K_{44} value indicates a decrease in oxygen affinity for the oxy state of about 2-fold between pH 7 and 6.5. Such a change would necessitate the presence of more than 50% liganded deoxy-state tetramers.

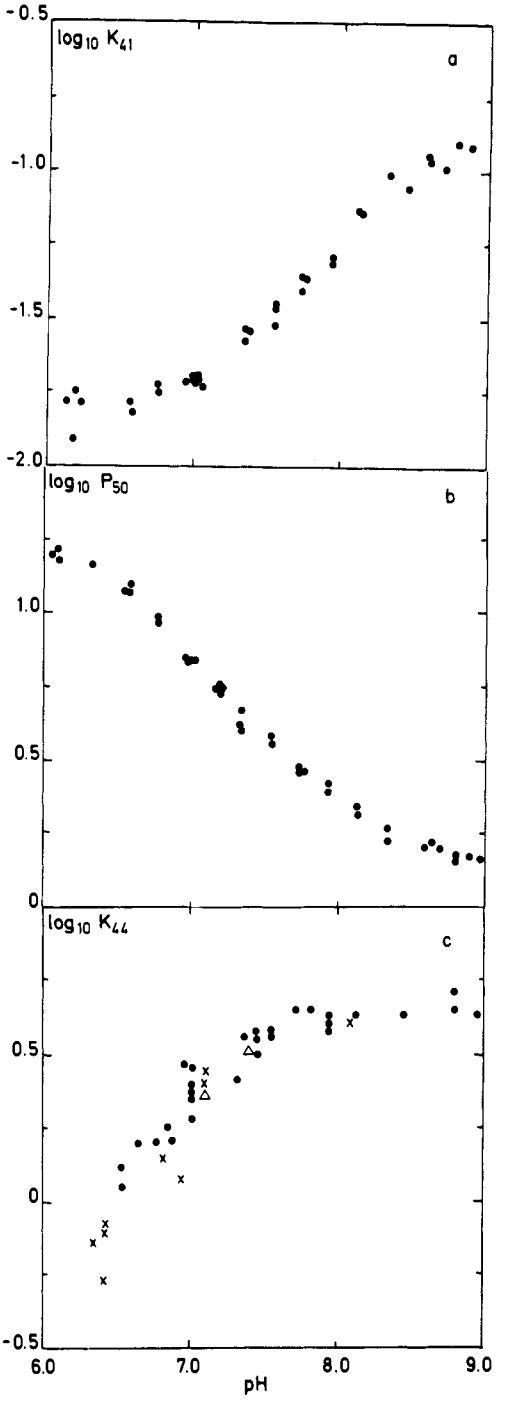

FIGURE 1: Experimental values for (a) log K_{41}, (b) log P_{50}, and (c) log K_{44} measured in purified HbA solutions (see text) with 50 mM Bis-Tris or Tris buffer and 0.1 M NaCl at 25 °C. The heme concentration was 0.7–0.8 mM in (a) and (b) and for the dots in (c). Crosses (×) and triangles (△) in (c) were at 7.15 and 16 mM heme, respectively.

Analysis of Experiments

In this section we apply the SKL model to a variety of experimental data. First, we outline results obtained utilizing only oxygen binding curves for hemoglobin A at two pH values (Roughton & Lyster, 1965) or at a series of pH values (Chu et al., 1984). It is now known that the pioneering measurements of Roughton and Lyster were made with unspecified solution conditions, so there is an uncertainty concerning the significance of their results. Nevertheless, we include fits to their data here, in part to permit comparison with the original SK model fits and in part to illustrate the sensitivity of measurements and model parameters to the solution conditions.

For the Roughton and Lyster (1965) and Chu et al. (1984) data, we restrict ourselves to two limiting cases of the SKL model. In particular, we consider the extended SK model, which has the salt-bridge coupling used in the original SK formulation, and the MWC type model, which has the salt bridges coupled purely to quaternary structure. As we demonstrate, it is not possible to distinguish these very different physical models without additional information. The necessary information can be obtained from the accurate ΔH_1^+ and ΔH_4^+ values given in the previous section. By using them we are able to proceed to an analysis of the salt-bridge coupling, as defined by the parameters r and r' in the SKL model.

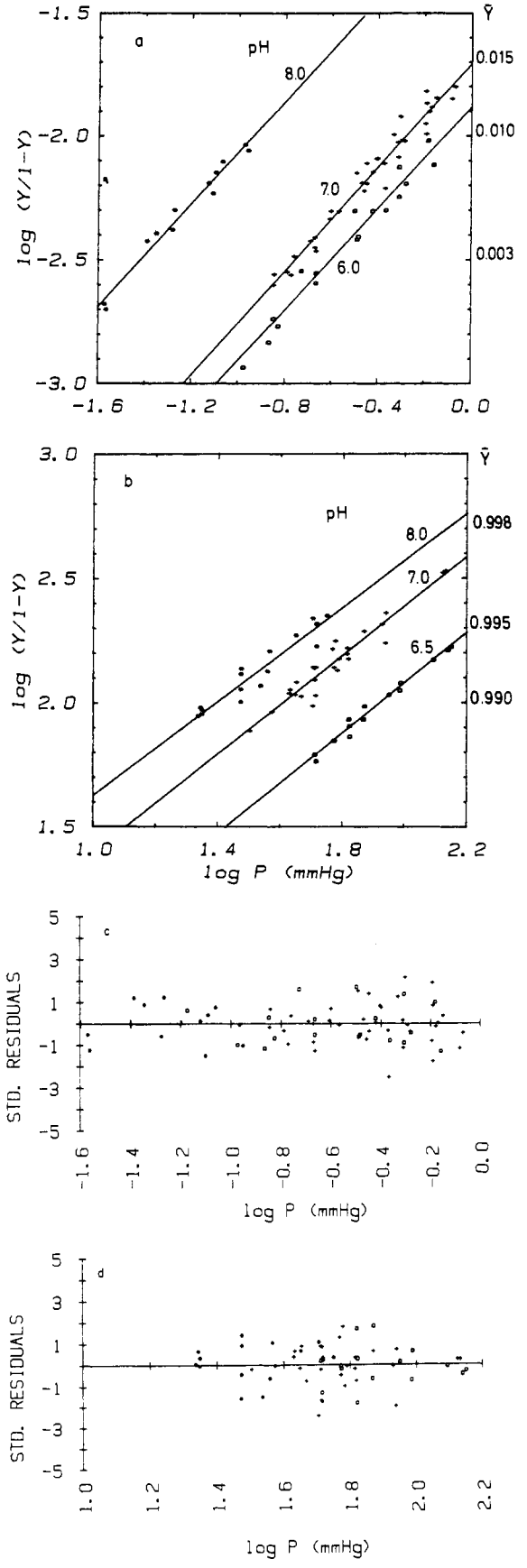

FIGURE 2: log $[\langle y_{O_2}\rangle/(1-\langle y_{O_2}\rangle)]$ vs log P values for the determination of (a) log K_{41} and (b) log K_{44}. Each symbol corresponds to an experimental point measured at a given pH at the conditions described under Experimental Results for ΔH_1^+ and ΔH_4^+. Solid lines are the calculated regression lines (Table I). Residuals (c and d) of the best fits for the three sets of experimental values shown in (a) and (b), respectively, with the same symbols for the different pH values.

(*A*) *Parameter Sets Used.* For the purpose of illustrating the pH behavior of the different models, we have utilized the parameter sets that are summarized in Table II. Parameter sets A and B have been obtained by least-squares fitting of the extended SK or MWC model to the Roughton–Lyster data (Roughton & Lyster, 1965) on human hemoglobin at pH 7 and 9.1 (Lee, 1984). For set A, pK^α is fixed at 7.5 and pK^β at 6.2, which are the values used in the original SK analysis. For set B, pK^α is 7.5, while pK^β is 7.0; the value for pK^β is that from the NMR measurements of Kilmartin et al. (1973). Parameter set C, which also corresponds to the extended SK and MWC limits, was determined by first using Bohr proton release data (Antonini et al., 1965) to estimate S, pK^α, and pK^β (Lee & Karplus, 1983) and then fitting the pH 7.4 oxygenation data generated with the tetramer Adair constants reported by Mills et al. (1976) to estimate Q, K_D^α, K_D^β, K_O^α, and K_O^β. For set D, a corresponding procedure was used except that r was allowed to vary to fit the ΔH_1^+ results. Sets C and D have lower pK^β values than sets A and B. This suggests that the pK of β His-146 is significantly lower (pK^β = 6.2) at diminished ionic strength in the absence of phosphate than in the presence of phosphate (pK^β = 7.0); no experimental value is available. As to pK^α, which is associated with α Val-1 in liganded hemoglobin, recent measurements yield values in the range 6.9–7.25 (Garner et al., 1975; Perrela et al., 1977; Van Beek, 1979); these are again lower than the value used to fit the Roughton–Lyster results and in accord with those used here for the model in the absence of phosphate. In the analysis of the experimental ΔH_1^+ and ΔH_4^+ data, we utilize the values of S, pK^α, and pK^β from sets C and D because the present measurements and those by Mills et al. (1976) were performed under similar solution conditions in the absence of phosphates. However, it should be noted that, in the experiments reported here, the concentration of Cl^- was kept at 0.1 M for all pH values studied, while the Cl^- concentration in the measurements of Mills et al. (1976) and Chu et al. (1984) varied over the range 0.1–0.2 M; this can have a small but nonnegligible effect on the results (Lee, Poyart, Bursaux, and Karplus, unpublished results). The Roughton–Lyster data, on the other hand, were obtained under very different conditions; the pH 7 measurements were carried out in 0.6 M inorganic phosphates, while the pH 9.1 measurements were in 0.2 M borate (Roughton & Lyster, 1965).

(*B*) *pH Dependence of Adair Constants.* Figure 3 shows the sequential Adair constants K_{4i}' plotted as a function of pH. In Figure 3a,b, the K_{4i}' have been calculated by using the extended SK and MWC values of parameter set A (based on the Roughton–Lyster data), while in Figure 3c,d the K_{4i}' have been calculated with parameter set C (based on the Mills et al. and Antonini et al. data). With the extended SK model and parameter set A, all of the constants are found to vary with pH (Figure 3a). The slope of K_{41}' is approximately constant between pH 8 and 10, K_{44}' is almost invariant above pH 8.5, and K_{42}' and K_{43}' vary the most with pH. The trends are similar for parameter set C (Figure 3c) except that K_{42}' does not vary as strongly with pH. For the MWC limit, interesting features (Figure 3b,d) include the slight degree of pH dependence exhibited by K_{41}' at alkaline pH (parameter set A) and by K_{44}' at acid pH (parameter set C). In this model, the observed proton release at the first ligation step must arise from the titration of the allosteric constant (eq 8b). To achieve this, a significant fraction of the singly liganded species must exist in the oxy quaternary structure at alkaline pH's (i.e., $L_1 \gg 1$ is not valid). Such a model has recently been considered by Johnson et al. (1984); see Discussion and

Table III: Calculated and Experimental Free Energies (kcal/mol) Corresponding to Adair Constants at Several pH's

	experimental[a]				extended SK model			
pH	$\Delta G_{41}'$	$\Delta G_{42}'$	$\Delta G_{43}'$	$\Delta G_{44}'$	$\Delta G_{41}'$	$\Delta G_{42}'$	$\Delta G_{43}'$	$\Delta G_{44}'$
7.4	−5.43 ± 0.11	−5.54 ± 1.30	−6.96 ± 1.10	−9.16 ± 0.35	−5.46	−5.43	−7.68	−8.69
	−5.46[b]	−5.43[b]	−7.66[b]	−8.71[b]				
8.0	−5.85 ± 0.07	−5.42 ± 1.20	−8.16 ± 1.35	−9.48 ± 0.35	−5.91	−5.99	−8.27	−8.95
8.5	−6.06 ± 0.13	−6.66 ± 0.60	−7.77 ± 0.90	−9.36 ± 0.53	−6.15	−6.35	−8.59	−9.06
8.95	−6.04 ± 0.13	−6.61 ± 0.55	−7.89 ± 1.20	−9.26 ± 0.30	−6.25	−6.53	−8.73	−9.09
9.5	−6.00 ± 0.07	−6.99 ± 0.85	−8.81 ± 0.85	−9.19 ± 0.11	−6.29	−6.63	−8.79	−9.11

[a] From Chu et al. (1984), except where noted. [b] From Mills et al. (1976).

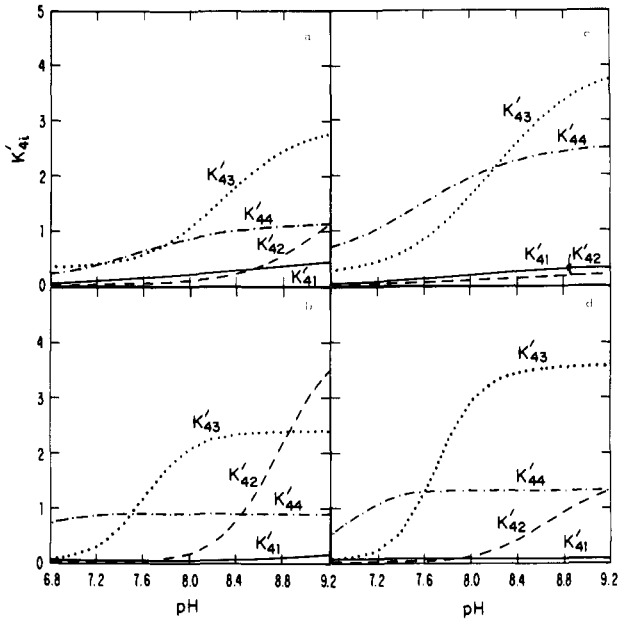

FIGURE 3: Plot of sequential Adair constants K_{4i}' vs pH: curves calculated (a) by using the extended SK fit with parameter set A, (b) by using the MWC fit with parameter set A, (c) by using the extended SK fit with parameter C, and (d) by using the MWC fit with parameter set C. Solid line for K_{41}', dashed line for K_{42}', dotted line for K_{43}', and dot-dashed line for K_{44}'.

Conclusions. The proton release at the last ligation step arises from the titration of L_4 (eq 12), so that at pH <7.5 a significant number of triply liganded tetramers must be present in the deoxy quaternary structure (i.e., $L_3 \gg 1$ is not valid).

The variation of K_{42}' and K_{43}' in the MWC model is substantially different from that in the extended SK model. In the former, proton release is linked only to a change in quaternary structure, as a result of which K_{42}' titrates mainly between pH 8 and 10, while K_{43}' varies over only 1 pH unit and is essentially invariant after pH 8. In the latter, proton release is either evenly partitioned between the second and third steps (parameter set A) or is confined primarily to the third step (parameter set C). The smaller pH dependence of K_{42}' with parameter set C is the result of the smaller pH-induced fractional change in the number of doubly liganded species with the deoxy quaternary structure. This is shown in Figure 4, where the fraction of n-liganded (n = 0–4) species in the deoxy or oxy state has been plotted as a function of pH. These results make clear that direct methods to evaluate the fraction of species present in different ligation states, particularly those with two or three ligands, are a very good way for distinguishing the different models.

Recently, Chu et al. (1984) have reported oxygenation data at several pH values between pH 7.4 and 9.5. Because of their interest in dimer properties, a large number of the measurements were made at low heme concentration where dimers are present in significant amounts. An extension of the SKL model

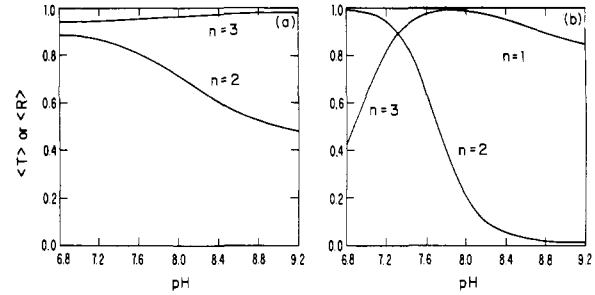

FIGURE 4: Fraction of n-liganded tetramers in the deoxy or oxy quaternary state vs pH calculated (a) by using the extended SK fit with parameter set C and (b) by using the MWC fit with parameter set C. For n = 0, 1, and 2 the fraction of molecules in the deoxy quaternary state, $\langle T \rangle$, is plotted; for n = 3 and 4 the fraction of molecules in the oxy quaternary state, $\langle R \rangle$, is plotted. Curves are not shown for the cases where the fraction is 1 within the resolution of the figure; e.g., for the extended SK fit, n = 0 and 1 are entirely in the $\langle T \rangle$ state and n = 4 is entirely in the $\langle R \rangle$ state.

to include dimers has been applied to the pH dependence of dimer–tetramer equilibria (Lee, 1984). However, the concern of this paper is with the properties of hemoglobin tetramers. Consequently, we restrict ourselves to comparing the tetramer Adair constants obtained from a previously determined parameter set (extended SK model with set C; Lee & Karplus, 1983) with those reported by Chu et al. (1984). The results are given in Table III. Comparison of theory with experiment shows that the agreement is within the quoted experimental uncertainties for most of the calculated values. The values for $\Delta G_{41}'$ ($= -RT \ln K_{41}'$) at pH 8.95 and 9.5 are just outside the given error ranges and may indicate that a somewhat larger r value is required to reproduce the experimental values than that corresponding to the extended SK model. However, it should also be noted that the parameter set used was not fitted to the Chu et al. (1984) pH dependence data but is that from a study based on the measurements of Antonini et al. (1965). Since the experimental conditions are not identical, it is possible that slightly different results would be obtained from a fit to Chu et al. (1984).

Two experimental entries have been included for pH 7.4 in Table III. The first set is from Chu et al. (1984), and the second set is from Mills et al. (1976). The most significant difference is a discrepancy of 0.45 kcal/mol between the two sets for $\Delta G_{44}'$ ($= -RT \ln K_{44}'$). This confirms that the Adair constants are sensitive to the choice of oxygenation data, which may be a reflection of systematic deviations in the dimer and dimer–tetramer equilibrium constants used in fixing the dimer contribution during data fitting. The value of −9.16 kcal/mol obtained by Chu et al. (1984) is somewhat surprising since other determinations in the literature do not reveal a value for $\Delta G_{44}'$ more negative than −9 kcal/mol: Imai (1979) reported a value of −8.64 kcal/mol at pH 7.4, 0.1 M Cl, and 21.5 °C; and Imaizumi et al. (1982) reported a value of −8.91 kcal/mol at pH 7.4, 0.1 M Cl, 25 °C, and 600 μM heme. From the present results (see Experimental Results for ΔH_1^+ and ΔH_4^+),

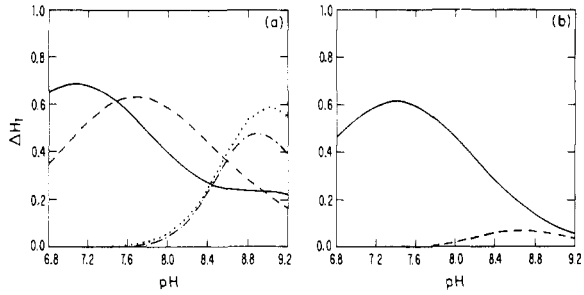

FIGURE 5: Limiting model results for ΔH_1^+ as a function of pH: (a) extended SK fit of parameter set A (solid line), extended SK fit of parameter set B (dashed line), MWC fit of parameter set A (dotted line), and MWC fit of parameter set B (dot-dashed line); (b) extended SK fit of parameter set C (solid line) and MWC fit of parameter set C (dashed line).

a value of −8.51 kcal/mol at pH 7.38, 25 °C, 0.1 M Cl, and 500–800 μM heme is obtained.

(C) Analysis of the Experimental ΔH_1^+ Curve for the Determination of r. (1) Extended SK versus MWC Models. Figure 5 shows the plot of ΔH_1^+ as a function of pH for the limiting extended SK and MWC models calculated with the parameter sets from Table I. For the extended SK fit with parameter set A, the pH at which maximal ΔH_1^+ (0.72 proton) occurs is approximately 7.3; there is also a shoulder at pH 9. The almost biphasic shape of this curve is due to the fact that more than 1 unit separates the pK values for the two Bohr groups, with the β chains titrating in the pH 7–8 region and the α chains in the pH 8–9 region. When pK^β is raised to 7.0 (parameter set B), a smooth bell-shaped curve results, with a maximum at pH 7.8. In this case, the majority of the contributions comes from the β chains since $K_D^\beta > K_D^\alpha$ and the internal salt bridge of the β chains titrates in the neutral–alkaline pH range. With the MWC fit of parameter set A, the pH profile is found to be centered at pH 9, where the α chains are the main contributors; contributions from the β chains increase when pK^β is raised to 7.0. With the extended SK fit of parameter set C, ΔH_1^+ is calculated to have a maximum of 0.62 proton at pH 7.4, with most of the contributions coming from the β chains ($K_D^\beta > K_D^\alpha$). The shoulder found with parameter set A has disappeared. With the MWC fit of parameter set C, ΔH_1^+ is calculated to be virtually zero in the pH range of interest.

It is important to note the difference in behavior of ΔH_1^+ for the different parameter sets in the MWC limit, where the salt bridges are linked to the quaternary structural change. The results make clear that a pH-dependent K_{41}' does not necessarily imply that the Bohr groups are tertiary-linked, which is the usual interpretation. From the expression for ΔH_1^+ in the MWC limit (eq 8b), it is seen that the magnitude of ΔH_1^+ depends on the pK's of the Bohr groups. Thus, the MWC fit of parameter set A (pK^α = 7.5) predicts a significant proton release at pH 9, while the MWC fit of parameter set C (pK^α = 6.96) predicts little proton release. Exactly how alkaline the pK's have to be for ΔH_1^+ to be nonnegligible depends on the values of the other parameters. The difference in behavior also makes evident the importance of accurate ΔH_1^+ measurements for distinguishing among the various models (see below).

(2) Validity of Approximate Equations (Eq 8a and 8b). The applicability of eq 8a as an approximation to ΔH_1^+ in the extended SK limit requires the validity of the assumption $L_1 \gg 1$. Figure 4 shows that the extended SK fit of parameter set C predicts the singly liganded species to exist almost exclusively in the deoxy quaternary state; hence, the assumption $L_1 \gg 1$ is valid for the entire pH range of interest (6.8–9.2). Analogous plots for the parameter sets A and B (not shown) indicate that the assumption begins to break down for them at pH >8.75. The applicability of eq 8b, which is exact in the MWC limit, to cases where r and r' deviate from the limiting values of $r = 1$ and $r' = 1/S$ also depends on the validity of the $L_1 \gg 1$ assumption. For the MWC fit of parameter set C, the assumption starts to break down at pH >8.5 ($L_1 < 10$), and for parameter sets A and B, the breakdown occurs at pH >8.25. However, $\partial \log K_{41}^D/\partial$pH and $\partial \log K_{41}^O/\partial$pH (eq 7b) are both expected to be small in this pH range for r and r' values not significantly different from the MWC values. Thus eq 8b should remain a good approximation.

Using the extended SK fit of parameter sets A and C, we tested eq 8a for a number of r values and found that the calculated ΔH_1^+ values between pH 6.0 and 9 agree very well with those from the exact expression. For both parameter sets, values of pH_{max} and $(\Delta H_1^+)_{max}$ calculated by using the approximate expression are correct to within 0.05 pK unit and 0.005 proton, respectively, either when r is varied between $1/S$ and 1, keeping $r' = 1$, or when r' is varied over the same range, keeping $r = 1/S$. Equation 8a also gives excellent agreement for intermediate values of r and r' (e.g., $r = 0.5$, $r' = 0.1$). The only situation in which eq 8a is not a good approximation in the extended SK limit is when certain MWC fits of the parameter sets are used. Then, it is possible that $L_1 \ll 1$ and the contribution from $\partial \log L/\partial$pH becomes dominant.

With the values for pK^α and pK^β that we have used (6.2–7.5), the results of Figure 5 show that if the experimental ΔH_1^+ curve peaks in the pH 7–8 range, then eq 8a (extended SK limit) is applicable; if the curve peaks between pH 8.5 and 9, then eq 8b (MWC limit) is applicable. Finally, if ΔH_1^+ is negligible throughout the pH range of interest, then the MWC model with pK's in the neutral range is applicable.

(3) Comparison with Present Measurements. Experimentally, the pH dependence of K_{41}' is unequivocal (Roughton & Lyster, 1965; Imai & Yonetani, 1975; Chu et al., 1984). Here we use the accurate experimental results between pH 6 and 9 reported in this paper (see Experimental Results for ΔH_1^+ and ΔH_4^+). Since the measurements were made at 500–800 μM heme concentration, the dimer concentration is negligible and the tetramer model can be employed directly. The values of K_{41}' as a function of pH have been obtained from the lower asymptotic region of the Hill plot (see Experimental Results for ΔH_1^+ and ΔH_4^+). To determine the corresponding proton release curve, the log K_{41} vs pH data have been fitted to a function of the form

$$\log K_{41} = B_0 + \log \frac{1 + \mu B_1 + \mu^2 B_2}{1 + \mu B_3 + \mu^2 B_4} \qquad (14)$$

where μ is the hydroxyl ion concentration. This is, in fact, the form of the expression for $\log K_{41}^D$ in eq 7b. An excellent fit obtained with eq 14 is shown in Figure 6a; the corresponding proton release curve calculated with the analytic derivatives of this fit is shown as the solid line in Figure 6b. The maximal proton release $(\Delta H_1^+)_{max}$ of 0.5–0.6 proton occurs between pH 7.5 and 7.7. Comparison of the experimental curve with the calculated ΔH_1^+ plots shown in Figure 5a,b indicates that the present results correspond closely to the extended SK model and that the MWC limit is not consistent with the measurements. The calculated curve for parameter set C is in good agreement with the experimental data.

Chu et al. (1984) have also estimated ΔH_1^+ between pH 7.4 and 9.5 from their Adair constants by fitting a function of the form $a + b(\text{pH}) + c(\text{pH})^2$ to $\Delta G_{41}'$. Such a function gives rise to a proton release curve ($\partial \log K_{41}'/\partial$pH = −(1/

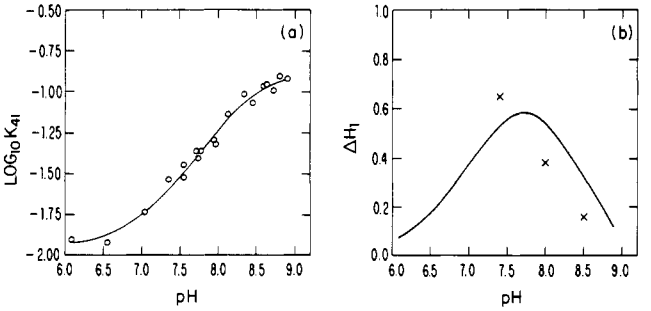

FIGURE 6: Fit of present data for K_{41} by eq 14 and determination of ΔH_1^+: (a) open circles represent data from Figure 1a, and the solid line is generated by using best-fit parameter values $B_0 = -1.969$, $B_1 = 6.852$, $B_2 = 10.842$, $B_3 = 5.689$, and $B_4 = 10.008$; (b) proton release curve (ΔH_1^+) calculated by using the derivatives of the best-fit parameter set in (a); crosses represent data from Chu et al. (1984) (see text).

$RT)\partial\Delta G_{41}'/\partial$pH) that is linearly dependent on pH. Thus, it cannot be used to describe the shape of the log K_{41}' vs pH curve over the entire pH range of interest and may explain why their estimated proton release at pH 8.95 is negative (i.e., proton uptake). Their reported ΔH_1^+ values are included in Figure 6b; they appear to be displaced by about 0.5 pH unit to lower values from the present results. The origin of this difference is not clear, though it may be due in part to the difference in overall Cl^- concentration (see above).

Effect of Chain Heterogeneity. To examine the dependence of ΔH_1^+ on chain heterogeneity, the value K_D^β/K_D^α is varied systematically. With the parameter sets of Table II and eq 8a, the pH profile was calculated for $0.1 \leq K_D^\beta/K_D^\alpha \leq 10$, and $r = 1/S$ (results not shown). As was pointed out above for parameter set A (Figure 5a), chain inequivalence exerts an influence on proton release only when the two pK's are substantially different. When $K_D^\beta/K_D^\alpha > 1$, the contribution from the internal β-chain salt bridges (maximum at pH $\approx$7) is increased relative to that calculated for $K_D^\alpha = K_D^\beta$, while that from the α chains (maximum at pH $\approx$8.5) is diminished. The converse is true when $K_D^\beta/K_D^\alpha < 1$. When proton release is calculated for parameter set C, $(\Delta H_1^+)_{max}$ is found to be quite constant at 0.62 proton, with pH_{max} occurring between pH 7.4 and 7.6, despite a 10^2-fold variation in K_D^β/K_D^α.

Effect of Varying r. When r is increased, which diminishes the coupling of the salt bridges to tertiary structure, $(\Delta H_1^+)_{max}$ decreases and pH_{max} shifts to more alkaline regions. For both parameter sets A and C, $(\Delta H_1^+)_{max}$ is less than 0.4 when r is larger than $S^{-0.5}$. Since the experimental results show $(\Delta H_1^+)_{max}$ to be $\approx$0.6 proton at pH $\approx$7.6, the salt bridges must be at least partially coupled to tertiary structural changes on ligation to explain the pH dependence of K_{41}. If the experimental curve is assumed to be characterized by $pH_{max} = 7.6 \pm 0.2$ and $(\Delta H_1^+)_{max} = 0.5 \pm 0.1$, values for r and K_D^β/K_D^α in the range $0 \leq \ln rS/\ln S \leq 0.2$ and $0.1 \leq K_D^\beta/K_D^\alpha \leq 10$ are found to give satisfactory agreement when values for S, pK^α, and pK^β from parameter set C are used. When the ΔH_1^+ curve calculated with S, pK^α, and pK^β from parameter set A and with $r = 0.042$ and $K_D^\alpha/K_D^\beta = 0.53$ is compared, the calculated ΔH_1^+ is overestimated by $\approx$0.1 proton at pH >8.5 and underestimated by the same amount at pH $\approx$7.8. For parameter set B, it has not been possible to obtain a value of S that reproduces the Bohr data.

If eq 8a is explicitly fitted to the experimental proton release curve (Figure 6), excellent agreement (root mean square $\approx$ 0.03) results with parameter values in the ranges $0.07 \leq r \leq 0.08$ and $0.05 \leq K_D^\beta/K_D^\alpha < 0.1$ (solid line, Figure 7). A slightly worse fit results with $K_D^\beta/K_D^\alpha > 1$ (dashed line, Figure

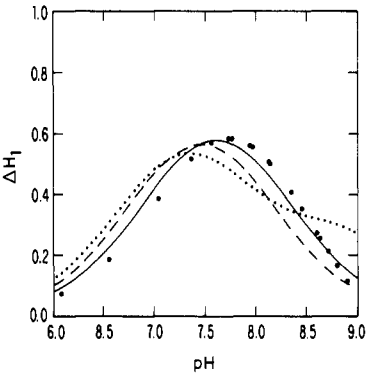

FIGURE 7: Model results for ΔH_1^+: (open circles) data from experiment; (solid line) best fit with $K_D^\beta/K_D^\alpha = 0.08$; (dashed line) best fit with $K_D^\beta/K_D^\alpha = 7.0$ (pK^α = 6.96; pK^β = 6.75; $-RT \ln S = -1.69$ kcal/mol); (dotted line) best fit with $K_D^\beta/K_D^\alpha = 0.53$ (pK^α = 7.5; pK^β = 6.2; $-RT \ln S = -2.15$ kcal/mol).

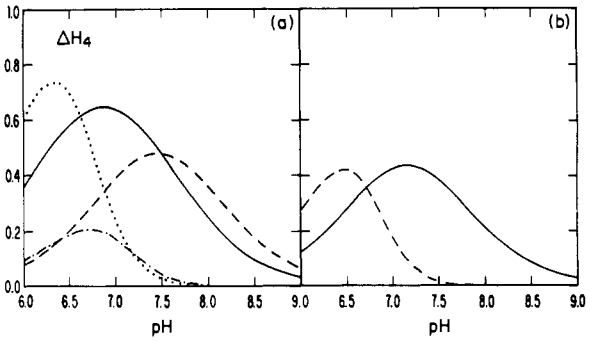

FIGURE 8: Limiting model results for ΔH_4^+ as a function of pH: (a) extended SK fit of parameter set A (solid line), extended SK fit of parameter set B (dashed line), MWC fit of parameter set A (dotted line), and MWC fit of parameter set B (dot-dashed line); (b) extended SK fit of parameter set C (solid line) and MWC fit of parameter set C (dashed line).

7) where the curve is shifted to the acid range by $\approx$0.2 pH units. Whether such a difference is significant is not clear. A curve calculated with pK^α, pK^β, and S from parameter set A and best-fit values for r (0.042) and K_D^β/K_D^α (0.53) is included in Figure 7 (dotted line). It is seen that beyond pH 7.2 the calculated ΔH_1^+ does not fit the experimental data.

The ΔH_1^+ curve calculated for the SK model with unequal strengths for titrable and nontitrable salt bridges (Lee & Karplus, 1983) is quite similar to that for the extended SK fit of parameter set C. Such a finding is to be expected since ΔH_1^+ depends only on S, the strength of the titrable group in the limit that $L_1 \gg 1$ (eq 8a).

(D) Analysis of the Experimental ΔH_4^+ Curve for the Determination of r'. (1) Extended SK versus MWC Model. Figure 8 shows the pH dependence of ΔH_4^+ calculated for the limiting models considered in this paper. The most important observation is that a pH-dependent K_{44}' is predicted for *both* the extended SK and MWC models; the differences lie in the details of the pH profile. In the extended SK model, the major contribution to the pH dependence of K_{44}' comes from the β chains since the quaternary structural change has taken place and the $\alpha_1\alpha_2$ salt bridges have been broken. For parameter set A, ΔH_4^+ peaks around pH 6.8–7 (pH_{max}), with a magnitude $[(\Delta H_4^+)_{max}]$ of 0.5–0.65 proton (Figure 8a, solid line). For parameter set B, pH_{max} is shifted to the more alkaline regions (pH 7.3–7.5) and $(\Delta H_4^+)_{max}$ decreases to 0.3–0.45 proton (Figure 8a, dashed line). For parameter set C, $(\Delta H_4^+)_{max}$ is equal to 0.4 proton and occurs at pH 7.2 (Figure 8b). In the case of the MWC model, the pH dependence of K_{44}' arises from the quaternary transition that accompanies binding of

the fourth ligand. The ΔH_4^+ curve is more sharply peaked than that calculated for the extended SK model, as a consequence of the strong pH dependence of the equilibrium between the deoxy and oxy quaternary contributions to $Hb(O_2)_3$ (Figure 4). With parameter set A, $(\Delta H_4^+)_{max}$ occurs at pH 6.4 and is equal to 0.7 proton (Figure 8a, dotted line). For parameter set B, $(\Delta H_4^+)_{max}$ is reduced to 0.2 proton (Figure 8a, dot-dashed line). For parameter set C, $(\Delta H_4^+)_{max}$ is equal to 0.4 proton and occurs at pH 6.5 (Figure 8b, dashed line).

Thus, in contrast to K_{41}', for which the differences between the extended SK and MWC models are well resolved for all the parameter sets considered, it is more difficult to distinguish between the two models based on the pH dependence of K_{44}'. Even though 0.5 pH unit separates $(\Delta H_4^+)_{max}$ in the two models, this difference occurs in the acid range, where contributions from the acid Bohr groups that have not been included in the model are likely to influence both pH_{max} and $(\Delta H_4^+)_{max}$. Thus, very accurate measurements and a more complete model are required for meaningful conclusions.

(2) Validity of Approximate Equations (Eq 11a and 12). The approximation for ΔH_4^+ in the extended SK limit requires the validity of the assumptions $L_4 \gg 1$ and $L_3 \gg 1$, while that for ΔH_4^+ in the MWC limit depends only on the applicability of $L_4 \gg 1$. A survey of all the cases treated in this paper indicates that the assumption $L_4 \gg 1$ is valid in the pH range of interest (pH 6–9), provided that the values of Q, K_D^α/K_O^α, and K_D^β/K_O^β are appropriate for the r and r' values considered. On the other hand, the assumption $L_3 \gg 1$ is applicable in the pH range of interest only when $r' > 1/S$. When $r' \approx 1/S$, as in the MWC model, the pH range for which $L_3 \gg 1$ is severely limited; i.e., the fraction of oxy quaternary tetramers $(L_3/L_3 + 1)$ decreases rapidly from a value near 1 at pH 7.8 to 0.4 at pH 6.8.

Equation 11a has been tested in the extended SK limit for parameter sets A and C. Its applicability is closely related to the value of r. When $\ln rS/\ln S \leq 0.2$, eq 11a is found to yield good agreement with the exact expression irrespective of the value of r' $(1/S \leq r' \leq 1)$. For cases at the upper limit of r, pH_{max} calculated with the approximate expression and parameter set A is the same as that found with the exact expression, while $(\Delta H_4^+)_{max}$ is slightly in error; e.g., for $r = 0.05$, $(\Delta H_4^+)_{max}$ is calculated to be 0.56 instead of 0.54. For parameter set C, $(\Delta H_4^+)_{max}$ is overestimated by 0.06 proton when $r = 0.1$; the approximate value of $(\Delta H_4^+)_{max}$ is 0.49. For values of r greater than $\ln rS/\ln S \approx 0.4$ (equivalent to $r = 0.13$ for parameter set A and $r = 0.2$ for parameter set C), the exact expression has to be used irrespective of the values of r'.

Equation 12 has been tested with the MWC fits from parameter sets A and C. It is found to give excellent agreement with the exact expression (Figure 8b). However, eq 12 appears to be a poor approximation when values of Q and the intrinsic affinities from the extended SK fit of parameter sets A and C are used, even in the MWC limit. This is true because the assumption $L_4 \gg 1$ is not valid with these parameter values. This is analogous to the situation described above for the case that parameter values from the MWC fit are used when ΔH_1^+ is approximated with eq 8a. We conclude that prior knowledge about r must exist in order to assess the validity of the assumption that $L_4 \gg 1$, since r in itself is the most important determinant of the magnitude of Q and the intrinsic affinities (for fixed values of pK^α and pK^β).

(3) Comparison with Present Measurements. Survey of Experimental Data. Just as r determines to a large extent the pH dependence of the first Adair constant, r' plays a major role in the proton release associated with the last oxygenation step. However, in contrast to the situation for K_{41}', the experimental data pertaining to the pH dependence of K_{44}' are not unequivocal. Crystallographically, the $\alpha_1\alpha_2$, $\alpha_1\beta_2$, and internal β-chain salt bridges are seen in the unliganded deoxy structure (Fermi, 1975, 1984; Fermi & Perutz, 1981) but not in the met, carbonmonoxy, or oxy structures (Ladner et al., 1977; Baldwin, 1980; Shaanan, 1983), where the termini are reported to be relatively delocalized. Chemical reactivity studies on α Val-1, the other Bohr group in the Perutz model, concur with the crystallographic findings. Thus, the experimental evidence indicates that the salt bridges contributing to the alkaline Bohr effect are broken in the fully liganded oxy tetramer.

As K_{44}' is a measure of the affinity of the last oxygenation step, its pH behavior is dependent on the status of the Bohr groups in the triply liganded $Hb(O_2)_3$ and fully liganded $Hb(O_2)_4$ species. The pH dependence of K_{44}' and thus the partial existence of the Bohr salt bridges in $Hb(O_2)_3$ are supported by the equilibrium oxygenation measurements of Roughton and Lyster (1965) and Imai (1979) and the data reported in the experimental results section. The experiments of Roughton and Lyster are complicated by the presence of 2,3-diphosphoglycerate (DPG), inorganic phosphates, and high ionic strength, but those of Imai and the present paper have been performed under standard conditions (0.1 M Cl^- and no DPG). Our measurements have been performed over a wide pH range (6.5–9.0), and a special effort has been made to reach the limiting asymptotic values of oxygen pressure. Although some inacuracies may be associated with the actual proton release curve ($\partial \log K_{44}'/\partial pH$) because of oxidation at the heme site, the data show clearly that K_{44}' is pH dependent (see below), with the largest change in the acid–neutral pH range. This conclusion is supported by the kinetic studies on the binding of the fourth carbon monoxide molecule by DeYoung et al. (1976) and by Kwiatkowski and Noble (1982) with respect to the pH dependence and to the maximal change at acid–neutral pH (pH 6–7.8). These measurements showed the dissociation rate constant for the fourth carbon monoxide (l_4) to range from $\approx 6.5 \times 10^{-3}$/s at pH 6 to $\approx 4 \times 10^{-3}$/s at pH 8 and for the association rate constant for the fourth carbon monoxide (l_4') to range from $\approx 4.1 \times 10^6$ M^{-1} s^{-1} at pH 6 to $\approx 8.3 \times 10^6$ M^{-1} s^{-1} at pH 9. These values of l_4 and l_4' imply that the affinity of hemoglobin for the fourth carbon monoxide ranges from $\approx 0.64 \times 10^9$/M at pH 6 to $\approx 2.05 \times 10^9$/M at pH 9.0.

There also exist data in the literature which indicate that K_{44}' is not pH dependent. There are the pH 6.5–8.8 oxygen saturation measurements of Imai and Yonetani (1975) and the pH 7.4–9.5 oxygen saturation measurements of Chu et al. (1984). The origin of the difference in the results of Imai (1979) and Imai and Yonetani (1975) concerning the pH dependence of K_{44}' is not clear. It is possible that the low hemoglobin concentration, leading to a mixture of dimers and tetramers, and the presence of 0.1 M phosphate [phosphate is a known allosteric effector; see Imai et al. (1977)] in the earlier studies are responsible for errors in the measured pH dependence. With regard to the data of Chu et al. (1984), there is no discrepancy since the pH range investigated does not include the region where the maximum in ΔH_4^+ occurs.

If $Hb(O_2)_3$ exists primarily in the oxy quaternary structure (Figure 4), a pH-dependent K_{44}' implies that a Bohr proton involving salt bridge is only partially linked to the quaternary structure. Consideration of the X-ray results indicates that only the internal β-chain salt bridge is able to exist in the oxy

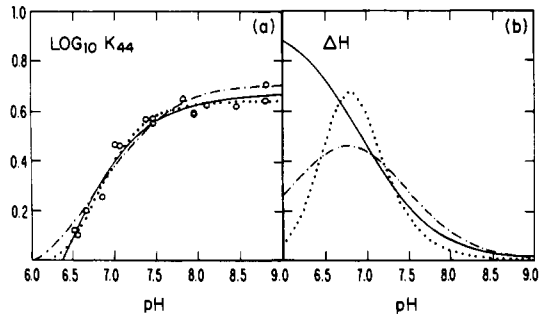

FIGURE 9: Fit of present data for K_{44} by eq 14 and determination of ΔH_4^+: (a) open circles represent data from Figure 1b; best fit with all data points weighted equally (solid line), best fit with entry at pH 6.6 deleted (dotted line), and fit with variance that is 2 times that of best fit (dot-dashed line); (b) proton release curves ΔH_4^+ calculated by using the derivatives of fits in (a).

quaternary structure. If, on the other hand, a significant fraction of $Hb(O_2)_3$ is in the deoxy state (as is the case when $r \approx 1$ at pH <8), a pH-dependent K_{44}' can arise from a pH-induced shift in the quaternary equilibrium for $Hb(O_2)_3$ with the β-chain Bohr group linked purely to the quaternary structure.

Comparison with Experiment. As with ΔH_1^+ we compare the model predictions to the ΔH_4^+ curve obtained from fits to the present data (Figure 9). Since it has not been possible to make measurements below pH 6.5, the slope of K_{44} in the range pH 6.5–7 is uncertain. This introduces difficulties since $(\Delta H_4^+)_{max}$ appears to occur in this region or at even lower pH values. With all the data points weighted equally (see Figure 9), the best fit yields a ΔH_4^+ curve that has a peak outside the range (i.e., below pH 6). However, because the experimental points do not extend below pH 6.5 and because the slope of the K_{44} curve appears to be still changing at this pH, $(\Delta H_4^+)_{max}$ and pH_{max} cannot be determined with certainty. For example, if a point at pH 6.6, which appears to be responsible for the continuing steep slope at pH 6.5, is removed from the data set, a fit statistically indistinguishable from the first yields a value of 0.7 proton for $(\Delta H_4^+)_{max}$ at pH 6.8 (see Figure 9). Another fit with a somewhat larger variance (see Figure 9) results in a curve with a value of 0.45 proton for $(\Delta H_4^+)_{max}$ at pH 6.8. Thus, depending on the particular weighting of the data points, a number of proton release curves with rather different pH profiles can be accommodated. For the purposes of the present analysis, we take $(\Delta H_4^+)_{max}$ to be 0.6 ± 0.3 proton and pH_{max} to be 6.5 ± 0.5.

Comparing the model results with experiment, we see that $(\Delta H_4^+)_{max}$ for the extended SK fit of parameter set C is shifted by ≈0.2 pK unit into the alkaline range beyond the upper limit of the observed pH_{max} (Figure 8b versus Figure 9). Equations 11b and 11c indicate that pH_{max} and $(\Delta H_4^+)_{max}$ can be adjusted by varying K_O^β/K_O^α and r'. The exact choice reflects a compromise between increasing K_O^β/K_O^α and decreasing r' to keep pH_{max} near 6.5–7 versus decreasing K_O^β/K_O^α and increasing r' to keep $(\Delta H_4^+)_{max}$ near the "observed" value of ≈0.4–0.6 proton. By decreasing r' from 1 to 0.6, pH_{max} is shifted from 7.2 to 7.05 and $(\Delta H_4^+)_{max}$ is decreased from 0.43 to 0.34 proton. Increasing r increases $(\Delta H_4^+)_{max}$ but does not shift pH_{max} significantly. The acceptable range for K_O^β/K_O^α depends on the value of the pH_{max} being fitted and on the values of the other model parameters. Assuming that pH_{max} occurs at ≈7, which is the upper limit of the range of pH_{max} suggested by the present data (Figure 9), and using the values of the pK's and S in parameter set A, we have found that K_O^β/K_O^α must be ≤0.1 in order to keep $r' \leq 1$. However, K_O^β/K_O^α needs only be <10.0 when parameter set C is used.

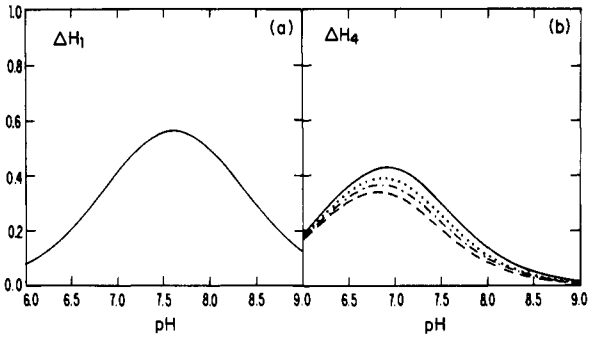

FIGURE 10: Calculated curves for ΔH_1^+ and ΔH_4^+ for parameter set D ($pK^\alpha = 6.96$; $pK^\beta = 6.51$). (a) ΔH_1^+. (b) Effect of varying r' on ΔH_4^+: (solid line) best fit; (dotted line) $r = 1/S$, $r' = 0.8$; (dot-dashed line) $r = 1/S$, $r' = 0.7$; (dashed line) $r = 1/S$, $r' = 0.6$.

If pH_{max} is ≈6.7, which is more likely (Figure 9), the pH profile is better fitted with a more acidic value for pK^β. For this purpose, the calculations have been repeated with a parameter set for $pK^\alpha = 6.96$ and $pK^\beta = 6.51$ [parameter set D in Table II; see also Lee and Karplus (1983)], which is a best fit to both the Bohr data of Antonini et al. (1965) and the oxygenation data of Mills et al. (1976). With these values of the pK's and S, pH_{max} is shifted to 6.9 with a $(\Delta H_4^+)_{max} = 0.43$, which is in agreement with the present measurements (Figure 10b). The ΔH_1^+ curve is also found to be well-reproduced with $r = 0.075$ and $K_D^\beta/K_D^\alpha = 0.08$ (Figure 10a). Thus, this parameter set is able to reproduce all the experimental data considered in this paper.

It should be noted that the unequal strength salt-bridge model, which does fit the general pH dependence (Lee & Karplus, 1983), leads to a ΔH_4^+ value that is too small [$(\Delta H_4^+)_{max} \approx 0.32$] at a pH value that is too high (results not shown).

Discussion and Conclusions

In this paper we have used a statistical mechanical model for ligand binding by hemoglobin (Szabo & Karplus, 1972; Lee & Karplus, 1983) to explore in depth one aspect of the cooperative mechanism, namely, the coupling of the essential salt bridges to tertiary and quaternary structural change. The important new aspect of the analysis is the use of accurate data for Bohr proton release at the first and fourth oxygenation steps as a function of pH measured under controlled solution conditions. The extended model (SKL model) contains parameters that make it possible to vary the coupling of salt bridges from that in the original SK formulation (interchain salt bridges coupled to both tertiary and quaternary structural change) to the Monod–Wyman–Changeux limit (all salt bridges coupled only to quaternary structural change). Although the SK-type and MWC-type models can both fit the oxygenation and overall proton release data with appropriately chosen parameters, the MWC-type model cannot fit the variation of proton release with pH at the first oxygenation step. This means that it is necessary for the interchain salt bridges to be coupled closely to tertiary structural change in the deoxy quaternary structure. Thus, it is possible to exclude a MWC-type model from consideration; this can be done only because of the availability of detailed and accurate proton release data over a wide range of pH values.

For the internal β-chain salt bridge, the tertiary–quaternary coupling is not as clear. We have based our analysis on the measurements reported in this paper since they provide the most comprehensive results under well-defined experimental conditions. The present data indicate that K_{44}' is pH dependent in the range pH 6–7 with a release of approximately 0.4–0.8

proton. Comparison of these data with model calculations indicates that both extended SK and MWC models can explain the qualitative behavior of K_{44}'. In the SK-type model, ΔH_4^+ results from the breaking of the internal β-chain salt bridge as ligand binds to the β chain in the oxy quaternary structure; in the MWC-type model, ΔH_4^+ comes primarily from the shift in quaternary structure as oxygen binds to the triply liganded molecules. The lack of an unequivocal interpretation arises from the fact that a complete delineation of the Bohr proton release curve for the fourth oxygenation step includes the acid pH range (less than pH 6). This region is difficult to examine experimentally. Also, the present models do not include acid Bohr groups, whose structural identification is still unclear; β His-143 has been shown to make a significant contribution (Kilmartin & Perutz, 1980; Matsukawa et al., 1984).

The original SK formulation (Szabo & Karplus, 1972) was based on the Roughton–Lyster data for oxygenation curves at pH 7 and 9.1. It was found that the measurements could be fitted with a formulation in which salt bridges of equal strength provided the entire stabilization of the unliganded deoxy quaternary structure; that is, the salt bridges were the sole coupling mechanism between tertiary and quaternary structural change. It now appears that the Roughton–Lyster results, probably due to differences in solution conditions for the two pH values, corresponded to a significantly larger Bohr effect than that found in more recent measurements under controlled solution conditions. This requires that there be a pH-independent contribution to cooperativity. One possible source in the Perutz model is the salt bridges that do not involve Bohr protons. In fact, use of pH-dependent and pH-independent salt bridges that have different strengths makes it possible to fit the full oxygenation curve and its pH dependence (Lee & Karplus, 1983). However, the present results for the proton release on the fourth ligation step indicate that this type of model is inadequate. Instead, a source of constraints on the ligand affinity and tertiary–quaternary coupling that is independent of the salt bridges appears to be required. This is in accord with structural and spectroscopic data and is included in the extended SK (SKL) model used for the present analysis (Lee & Karplus, 1983). An essential element in the model is the inclusion of two different tertiary structures (liganded and unliganded) for each of the quaternary structures; this contrasts with the earlier SK model where the quaternary transition induced no change in tertiary structure, other than that involving the salt bridges. Such a generalization of the model leads directly to the possibility of constraints on ligand binding independent of the salt bridges and permits the formulation of the salt-bridge coupling to tertiary and quaternary structural change that has been verified in this paper.

It may be useful to contrast the structurally related statistical mechanical model used here with the procedure for fitting hemoglobin oxygenation and Bohr effect data reported recently by Johnson et al. (1984). Their model is based on the same set of tertiary and quaternary structures as the original SK model but differs in a number of ways. Most important is the fact that they assume that there is no tertiary contribution to the Bohr effect or, more exactly, that it is negligibly small; i.e., they use the measured Bohr effect for the dimer as that of the chains in the cooperative tetramer. This disagrees with our formulation and other data which suggest that in each quaternary structure of the tetramer tertiary structural change on ligation can lead to significant proton release that is different from that found in the isolated subunit or in the noncooperative dimer. It is just this tertiary–quaternary coupling and its pH dependence that we have explored in detail in this paper.

Johnson et al. (1984) are able to fit the Bohr data with pure quaternary coupling of the Bohr groups by redetermining 12 of the 13 parameters in their model at each pH. This corresponds to using an independent model for each pH, which as we have found makes it impossible to test the significance of the resulting fits. Compared to the extended SK model, which uses 9 parameters and includes the entire alkaline pH range in a consistent formulation, Johnson et al. (1984) used 49 parameters for the four pH values they studied (pH 7.4, 8.0, 8.5, and 8.95). Moreover, their "striking prediction" that 30% of the tetramers have the oxy quaternary structure when only singly ligated follows directly from their assumption that the Bohr effect is linked purely to quaternary structure. Such a MWC-type limit has been considered by us and appears to be inconsistent with the data for ΔH_1^+ reported in this paper.

In conclusion, it must be noted that any model for hemoglobin is an oversimplification. In fact, it is the essence of a model that it focuses on the essential aspects and neglects others that may become significant as new experimental data are obtained. The model we have described and tested here is consistent with the available information. We hope that it will serve as a basis for more detailed and refined descriptions that will be required to explain additional measurements. Particularly exciting is the possibility that a more fundamental understanding of the parameters used in the statistical thermodynamic model will result from forthcoming experimental and theoretical studies of natural and artificial mutants of the hemoglobin molecule (Nagai et al., 1985).

ACKNOWLEDGMENTS

We are grateful to M. Perutz for helpful comments on the manuscript. We thank G. Ackers for focusing our attention on the question of the range of applicability of the Szabo–Karplus model. We acknowledge the comments of a referee that led us to provide a full discussion of the Bohr proton assignments and to provide more detailed statistics for the experimental measurements.

Registry No. HbA, 9034-51-9; O_2, 7782-44-7.

REFERENCES

Adair, G. (1925a) *Proc. R. Soc. London, A 109*, 292–301.
Adair, G. (1925b) *J. Biol. Chem. 63*, 529–545.
Anderson, L. (1973) *J. Mol. Biol. 79*, 475–506.
Anderson, L. (1975) *J. Mol. Biol. 94*, 33–49.
Antonini, E., & Brunori, M. (1971) *Front. Biol. 21*, 135–152.
Antonini, E., Wyman, J., Brunori, M., Bucci, E., Fronticelli, C., & Rossi-Fanelli (1965) *J. Biol. Chem. 240*, 1096–1103.
Baldwin, J. (1980) *J. Mol. Biol. 136*, 103–128.
Brown, F., & Campbell, I. (1976) *FEBS Lett. 65*, 322–325.
Bunn, H., & Guidotti, G. (1972) *J. Biol. Chem. 247*, 2345–2350.
Chu, A., & Ackers, G. (1981) *J. Biol. Chem. 266*, 1199–1205.
Chu, A., Turner, B., & Ackers, G. (1984) *Biochemistry 23*, 604–617.
DeYoung, A., Penelly, R., Tan-Wilson, A., & Noble, R. (1976) *J. Biol. Chem. 251*, 6692–6698.
Dolman, D., & Gill, S. J. (1978) *Anal. Biochem. 87*, 127–134.
Edelstein, S. J. (1971) *Nature (London) 230*, 224–227.
Fermi, G. (1975) *J. Mol. Biol. 97*, 237–256.
Fermi, G. (1984) *J. Mol. Biol. 175*, 159–174.
Fermi, G., & Perutz, M. (1977) *J. Mol. Biol. 114*, 421–431.
Fermi, G., & Perutz, M. (1981) in *Atlas of Molecular Structures in Biology* (Phillips, D. C., & Richards, F. M., Eds.) Vol. 2, pp 35–55, Clarendon, Oxford, U.K.

Garner, H., Bogart, R., & Gurd, J. (1975) *J. Biol. Chem. 250*, 4398–4404.
Gelin, B., & Karplus, M. (1977) *Proc. Natl. Acad. Sci. U.S.A. 74*, 801–805.
Gelin, B., Lee, A. W.-M., & Karplus, M. (1983) *J. Mol. Biol. 171*, 489–559.
Hayashi, A., Susuki, T., & Shin, M. (1973) *Biochim. Biophys. Acta 310*, 309–316.
Imai, K. (1979) *J. Mol. Biol. 133*, 233–247.
Imai, K. (1982) in *Allosteric Effects in Haemoglobin*, pp 129–136, Cambridge University, Cambridge, U.K.
Imai, K., & Yonetani, T. (1975) *J. Biol. Chem. 250*, 2227–2231.
Imai, K., Yonetani, T., & Ikeda-Saito, M. (1977) *J. Mol. Biol. 109*, 83–97.
Imaizumi, K., Imai, K., & Tyuma, I. (1982) *J. Mol. Biol. 159*, 703–719.
Johnson, M., Halvorson, H., & Ackers, C. (1976) *Biochemistry 15*, 5363–5371.
Johnson, M. L., Turner, B. W., & Ackers, G. K. (1984) *Proc. Natl. Acad. Sci. U.S.A. 81*, 1093–1097.
Kilmartin, J., Breen, J., Roberts, J., & Ho, C. (1973) *Proc. Natl. Acad. Sci. U.S.A. 70*, 1246–1249.
Kilmartin, J. C., Imai, K., Jones, R. T., Faruqui, A. R., Fogg, J., & Baldwin, J. M. (1978) *Biochim. Biophys. Acta 534*, 15–25.
Kilmartin, J., Fogg, J., & Perutz, M. (1980) *Biochemistry 19*, 3189–3193.
Kirkwood, J., & Weistheimer, F. (1938) *J. Chem. Phys. 6*, 506–512.
Koshland, D., Nemethy, J., & Filmer, D. (1966) *Biochemistry 5*, 365–385.
Kwiatkowski, L., & Noble, R. (1982) *J. Biol. Chem. 257*, 8891–8895.
Ladner, R., Heidner, E., & Perutz, M. (1977) *J. Mol. Biol. 114*, 385–414.
Lee, A. (1984) Ph.D. Thesis, Harvard University, Cambridge, MA.
Lee, A., & Karplus, M. (1983) *Proc. Natl. Acad. Sci. U.S.A. 80*, 7055–7059.
Loukopoulos, D., Poyart, C., Delanoe-Garin, J., Matsis, C., Arous, N., Kister, J., Loustradi-Anagnostou, A., Blouquit, Y., Fessas, P., Thillet, J., Rosa, J., & Galacteros, F. (1986) *Hemoglobin 10*, 143–160.
Matsukuwa, S., Itatani, Y., Mawatani, K., Shimokawa, Y., & Yoneyama, Y. (1984) *J. Biol. Chem. 259*, 11479–11486.
Matthew, J., Hanania, G., & Gurd, F. (1979a) *Biochemistry 18*, 1919–1928.
Matthew, J., Hanania, G., & Gurd, F. (1979b) *Biochemistry 18*, 1928–1936.
Matthew, J., Gurd, F. R. N., Flanagan, M. A., March, K. L., & Shire, S. J. (1985) *CRC Crit. Rev. Biochem. 18*, 91–197.
Mills, F., & Ackers, G. (1979a) *Proc. Natl. Acad. Sci. U.S.A. 76*, 273–277.
Mills, F., & Ackers, G. (1979b) *J. Biol. Chem. 254*, 2881–2887.
Mills, F., Johnson, M., & Ackers, G. (1976) *Biochemistry 15*, 5350–5362.
Monod, J., Wyman, J., & Changeux, J. (1965) *J. Mol. Biol. 12*, 88–118.
Nagai, K., Perutz, M. F., & Poyart, C. (1985) *Proc. Natl. Acad. Sci. U.S.A. 82*, 7252–7255.
Ogata, R. T., & McConnell, H. M. (1972) *Proc. Natl. Acad. Sci. U.S.A. 69*, 335–339.
Ohe, H., & Kajita, A. (1980) *Biochemistry 19*, 4445–4452.
Perrella, M., Guglielmo, G., & Mosca, A. (1977) *FEBS Lett. 78*, 287–290.
Perutz, M. F. (1970a) *Nature (London) 228*, 726–734.
Perutz, M. F. (1970b) *Nature (London) 228*, 734–739.
Perutz, M. F., & Ten Eyck, L. (1972) *Cold Spring Harbor Symp. Quant. Biol. 36*, 295–310.
Perutz, M. F., Kilmartin, J. V., Nishikura, K., Fogg, J. H., Butler, P. J. G. & Rollema, H. S. (1980) *J. Mol. Biol. 138*, 649–670.
Perutz, M. F., Fermi, G., & Shih, F. B. (1984) *Proc. Natl. Acad. Sci. U.S.A. 81*, 4781–4784.
Perutz, M. F., Gronenborn, A. M., Clore, G. M., Fogg, J. H., & Shih, D. (1985a) *J. Mol. Biol. 183*, 491–498.
Perutz, M. F., Gronenborn, A. M., Clore, G. M., Shih, D. T., & Craescu, M. (1985b) *J. Mol. Biol. 186*, 471–473.
Poyart, C., Bursaux, E., & Bohn, B. (1978) *Eur. J. Biochem. 87*, 75–83.
Poyart, C., Bursaux, E., Arnone, A., Bonaventura, C., & Bonaventura, J. (1980a) *J. Biol. Chem. 255*, 9465–9473.
Poyart, C., Bursaux, E., & Matzke, P. (1980b) in *Biophysics and Physiology of Carbon Dioxide* (Bauer, C., Gros, G., & Bartels, H., Eds.) Springer, Berlin.
Roughton, P. W., & Lyster, R. L. (1965) *Hvalradets Skr. 48*, 185–201.
Russu, I. M., & Ho, C. (1986) *Biochemistry 25*, 1706–1716.
Russu, I. M., Ho, N., & Ho, C. (1980) *Biochemistry 19*, 1043–1052.
Russu, I. M., Ho, N., & Ho, C. (1982) *Biochemistry 21*, 5031–5043.
Shaanan, B. (1983) *J. Mol. Biol. 171*, 31–59.
Szabo, A., & Karplus, M. (1972) *J. Mol. Biol. 72*, 163–197.
Szabo, A., & Karplus, M. (1975) *Biochemistry 14*, 931–940.
Szabo, A., & Karplus, M. (1976) *Biochemistry 15*, 2869–2877.
Tanford, C., & Kirkwood, J. (1957) *J. Am. Chem. Soc. 79*, 5333–5339.
Van Assendelft, O. W. (1970) in *Spectrophotometry of Haemoglobin Derivatives*, pp 55–65, C. C. Thomas, Assen, The Netherlands.
Van Beek, G. (1979) Thesis, University of Nijwegen, The Netherlands.
Wyman, J. (1948) *Adv. Protein Chem. 4*, 407–531.
Wyman, J. (1964) *Adv. Protein Chem. 19*, 223–286.